Sasol Advanced Fuels Laboratory

UNIVERSITY OF CAPE TOWN

A Theoretical Assessment of Fuel Combustion Attributes to Enhance the Operational Envelope of HCCI Engines

Author:

Sibusiso C. Londleni

Supervised by:

Mr André Swarts and Prof. Andrew D. B. Yates

A dissertation submitted to the Department of Mechanical Engineering, University of Cape Town, in partial fulfilment of the requirements for the degree of Master of Science in Engineering

Cape Town, South Africa
31 March 2006

Declaration

1. Plagiarism is the illegal use another's work and pretending that it is one's own

2. I have used the Harvard convention for citation and referencing. Each significant contribution to, and quotation in, this project from the work(s) of other people has been attributed, and has been cited and referenced.

3. This project is my own work and has also not been submitted for any purpose or examination to any other Department or University.

4. I have not allowed, and will not allow anyone to copy my work with the intention of passing it off as his/her own work.

Signature:.. Signed by candidate

Date:..30/03/2006

Acknowledgements

This project was initiated and sponsored by:

sasol
reaching new frontiers

First and foremost, the author wishes to thank the Lord Jesus Christ for providing strength and courage even through difficult times to put this project to completion.

Also, the author wishes to thank the following people for their enormous help and contributions in making this project a success:

Mr. André Swarts – Project supervisor, and many thanks for being more than just a project supervisor, Sasol Advanced Fuels Laboratory (SAFL)

Prof. Andrew D. B Yates – Project co-supervisor, and your advices are highly appreciated, SAFL

Mr. Carl Viljoen – Assistance with Chemkin modelling and useful fuel data, SAFL

Prof. Hiroshi Kawanabe – Assistance with the burn duration correlation. Kyoto University. Japan

Mrs. Joey Swarts – For being a parent away from home and providing help when needed the most, HR personnel, SAFL

Mr. and Mrs. Tsana and the Members – For the prayers, encouragements and for becoming friends when it mattered most.

To all those who contributed directly or indirectly, and all those not mentioned your help highly is appreciated. *"May the good Lord, Jesus Christ richly bless you all."*

Abstract

Homogeneous Charge Compression Ignition (HCCI) is an alternative internal combustion (IC) engine that can provide high efficiencies while producing ultra-low nitrous oxides (NO_x) and particulate matter (PM) emissions compared to existing compression ignition (CI) and spark ignition (SI) engines. HCCI engines operate on the principle of having a dilute, premixed charge that reacts and burns volumetrically throughout the cylinder as it is compressed by the piston. The large amounts of charge dilution also dramatically reduce the peak burned gas temperatures resulting in low NO_x emissions. Since there is no fuel-rich diffusion burning taking place, the PM emissions are at near zero levels. In theory, HCCI combustion can be achieved with any fuel that evaporates readily and autoignite under the conditions typically found in an internal combustion engine.

In some regards, HCCI incorporates the best features of both SI and CI engine. As in a SI engine, the charge is well mixed, which minimises particulate emissions and as in a CI engine, the charge is compression ignited and has no throttling losses, which leads to high thermal efficiencies. However, unlike either of these conventional engines, the combustion occurs simultaneously throughout the combustion chamber without a flame front, eliminating the flammability limits associated with SI combustion. The HCCI engine can provide efficiencies as high as compression ignition engines while generating extremely low NO_x emissions, as low as 1-5% tailpipe NO_x of a conventional SI engine.

Lack of direct control of combustion phasing and a limited load and speed operating range are some of the barriers to overcome before HCCI engine technology can be brought to the market. Faced with the challenges of HCCI combustion and the demand for cleaner fuels, Sasol identified an opportunity for future business and funded this research project to develop a simple mathematical model that could be used as a tool to simulate HCCI combustion. In addition, a secondary aim was to explore fuel combustion characteristics that would enable HCCI operation over the full range of speed and load.

A simple mathematical model that could be used as a tool to simulate HCCI combustion was developed and validated against experimental data. Despite the relative simplicity of the model, it proved able to predict the start of combustion within reasonable accuracy. Moreover, the model produced results that were in good agreement with literature and available measurements.

The compression ratio was identified to be one of the most important parameters when designing a fuel for HCCI combustion. For example, if the fuel was designed for low compression ratios and used at high compression ratios engine knock would result and vice versa. With a suitable compression ratio it was possible to conceive fuel properties that could be operated through the load and speed range. The fuel allowed HCCI combustion throughout the speed range (1000 – 5000 rpm) and load range ($0.2 \leq \Phi \leq 1$) without any forced induction. However, high peak pressures and heat release rates appeared to be inevitable at high loads.

It was recommended to conduct an investigation on how much heat is released during cool flames and to confirm the association of the start of cool flames with the low temperature ignition delay. These findings need to be implemented in the model to improve the model predictions of combustion phasing of fuels with two-stage ignition.

It was further recommended to conduct more experiments and 3-D modelling with different engines using different fuels and operating conditions to establish data that can be used to refine the combustion duration correlation. Furthermore, it was recommended to match the ignition delay characteristics with different known fuels and blends to obtain the designer fuel thermodynamic and physical properties.

Contents

List of Figures

List of Tables

Nomenclature

Acronyms

ABDC	After bottom dead centre
ATDC	After top dead centre
BBDC	Before bottom dead centre
bMEP	Break mean effective pressure
BTDC	Before top dead centre
CA10	Crank angle of 10% heat release
CA90	Crank angle of 90% heat release
CAD	Crank angle degrees
CI	Compression ignition
CO	Carbon monoxide
CO_2	Carbon dioxide
CR	Compression ratio
DI	Direct injection
DME	Dimethyl ether
EGR	Exhaust gas recirculation
EVC	Exhaust valve closure
EVO	Exhaust valve opening
FBR	Full boiling range
fMEP	Friction mean effective pressure
H_2	Hydrogen
H_2O	Water
HC	Hydrocarbon
HCCI	Homogeneous charge compression ignition
IC	Internal combustion
IMEP	Indicated mean effective pressure
ISFC	Indicated specific fuel consumption
IVC	Inlet valve closure
IVO	Inlet valve opening
MBT	Maximum brake torque
MON	Motor octane number
NO_x	Nitrous oxides
NTC	Negative temperature coefficient

ON	Octane number
PM	Particulate matter
PRF	Primary reference fuels
RCM	Rapid compression machine
RON	Research octane number
RPM	Revolutions per minute
SAFL	Sasol advanced fuels laboratory
SI	Spark ignition
SOC	Start of combustion
TDC	Top dead centre
VCR	Variable compression ratio
VVA	Variable valve actuation
VVT	Variable valve timing

List of Symbols

A	Pre-exponential constant of proportionality
B	Cylinder bore
	Temperature coefficient
a	Wiebe function multiplier
b	Wiebe function exponent
E_a	Activation energy
F	Mole fraction of fuel
h_{conv}	Convection heat transfer coefficient
k	Rate constant
	Exponent of air-fuel ratio
m	Exponent of the exhaust gas recirculation
Md	Molecular density of the mixture
m_f	Mass of fuel
n	Pressure coefficient
O	Mole fraction of oxygen
p	Pressure
Q_{int}	Heat transfer through the intercooler
Q_{LHV}	Low heat value of fuel
R	Universal gas constant
S_p	Average mean piston speed

T	Temperature
t	Time
V_d	Displacement volume
W_c	Work done per cycle
W_{comp}	Compressor work
x_b	Mass fraction burnt
$\Delta\theta$	Combustion duration in crank angle degrees
η	Efficiency
θ	Crank angle
λ	Air-fuel ratio
Φ	Fuel-air equivalence ratio
τ	Ignition delay
τ_{cd}	Combustion duration in milliseconds

Subscripts

b	Burnt gas
c	Cycle
cd	Combustion duration
comb	Combustion
comp	Compressor
conv	Convection
corr	Corrected
d	Displaced
f	Fuel
i	Dummy index for 1, 2, 3
int	Intercooler
max	Maximum
mech	Mechanical
o	Overall
th	Thermal
u	Unburnt gas
m	Motored

1 Introduction

1.1 Project Background

The increasing demand for more power and efficiency by the consumers leads the engine manufacturers to improve engine designs. Moreover, the increasingly stringent legislative requirement on tail-pipe emissions by the government leads the fuel manufacturers to search for cleaner fuels. Further improvements of SI engines to meet the demands are limited by engine knock, an abnormal combustion phenomenon which depends on engine design and operating conditions, as well as the fuel. Knock is the ultimate constraint on spark ignition (SI) engine efficiency since it limits the compression ratio (Heywood, 1988). On the other hand, high levels of nitrous oxides (NO_x) and particulate matter (PM) emissions are the drawback in compression ignition (CI) technology.

Homogeneous Charge Compression Ignition (HCCI) technology has emerged over the past decade as an alternative internal combustion (IC) engine that has the potential to meet the abovementioned demands. This engine technology promises to dramatically reduce NO_x and PM emissions, whilst providing efficiency levels comparable to those of diesel engines. HCCI combustion involves an autoignition process that combines the best features of the SI and CI processes.

In a HCCI engine, the air and fuel are premixed homogeneously prior to ignition and then ignited by the compression from the piston motion. The ignition is ideally simultaneous and therefore the charge gives an instantaneous energy release (approaching Otto air standard cycle). This uniform and simultaneous autoignition occurs throughout the whole charge without flame propagation. There is no direct control of the start of combustion and the rate of heat release. As such, the combustion process is primarily controlled by chemical kinetics, which makes it very sensitive to the thermodynamic state of the mixture charge (Aroonsrisopon et al., 2002).

Like any other engine technology, HCCI engine posses its own set of unique challenges that include lack of control over combustion phasing and a limited load and speed operating range. There has been an increasing worldwide research and development of this engine

technology and attempts to overcome the challenges before the engine can be brought to the market.

1.2 Project Objectives

Faced with the challenges of HCCI combustion and the demand for cleaner fuels, Sasol identified an opportunity for a future business and funded this research project to:

- Develop a simple mathematical model that could be used as a tool to simulate HCCI combustion. However, it must demonstrate the potential to produce usable results.

- Validate the model using published experimental data. Study the fuel behaviour and the effect of fuel composition on HCCI combustion.

- Explore a designer fuel (refers to developing autoignition behaviour of a design fuel) that will work in the model engine over the full range of operation. If possible, relate the designer fuel to conventional fuel characteristics.

1.3 Plan of Development

This document is structured to enable the reader to follow the method of investigation. The following chapter gives the review of the relevant literature, particularly the development of HCCI engine technology and effect of fuels. Literature on modelling of fuel autoignition is also briefly discussed.

Chapter 3 describes the mathematical model of HCCI combustion and highlights the procedure followed in producing the results.

In Chapter 4, the results are presented and discussed. Finally, conclusions are drawn on the results and recommendations for future work are made on the basis of the conclusions.

2 Literature Review

2.1 HCCI Description

Homogeneous Charge Compression Ignition (HCCI) is an alternative internal combustion (IC) engine that can provide high efficiencies while, producing ultra-low nitrous oxides (NO_x) and particulate matter (PM) emissions compared to existing compression ignition (CI) and spark ignition (SI) engines. HCCI engines operate on the principle of having a dilute, premixed charge that reacts and burns volumetrically throughout the cylinder as it is compressed by the piston (U.S. Dep. of Energy, 2001). In theory, HCCI combustion can be achieved with any fuel that evaporates readily and autoignite under the condition typically found in an internal combustion engine.

In some regards, HCCI incorporates the best features of both SI and CI engine. As in a SI engine, the charge is well mixed, which minimises particulate emissions and as in a CI engine, the charge is compression ignited and has no throttling losses, which leads to high thermal efficiencies (Epping et al., 2002). However, unlike either of these conventional engines, the combustion occurs simultaneously throughout the combustion chamber without flame front, eliminating the flammability limits associated with SI combustion. HCCI engine can provide efficiencies as high as compression ignition engines while generating extremely low NO_x emissions, as low as 1-5% tailpipe NO_x of a conventional SI engine (Xu et al., 2002).

In general, HCCI engines operate very lean due to high levels of dilution, which control the energy release rates to within acceptable levels. The large amounts of charge dilution also dramatically reduce the peak burned gas temperatures resulting in much low NO_x emissions. Since there is no fuel-rich diffusion burning taking place, the PM emissions are at zero levels (Zhao et al., 2003).

2.2 Advantages of HCCI

The advantages of HCCI engine depend on the combustion system to which it is compared. Relative to SI engine, HCCI engines are more efficient, approaching CI efficiencies. This improvement is as a result of elimination of throttling losses; the use of high compression ratios similar to CI, and shorter burn duration since it is not necessary for flame propagation across the cylinder (Epping et al., 2002). HCCI engines produce lower NO_x emissions than SI engines without any exhaust after-treatment.

Relative to CI engines, HCCI engines have substantially lower emissions of PM and NO_x. Particulate matter and nitrous oxides emissions are major impediments to CI engines meeting future emissions standards and are the focus of extensive current research (U.S. Dep. of Energy, 2001). The low emissions of PM and NO_x in HCCI engines are as a result of the dilute homogeneous air and fuel mixture in addition to low combustion temperatures. So HCCI engines beat the PM-NOx trade-off in CI engines (see figure 2-1).

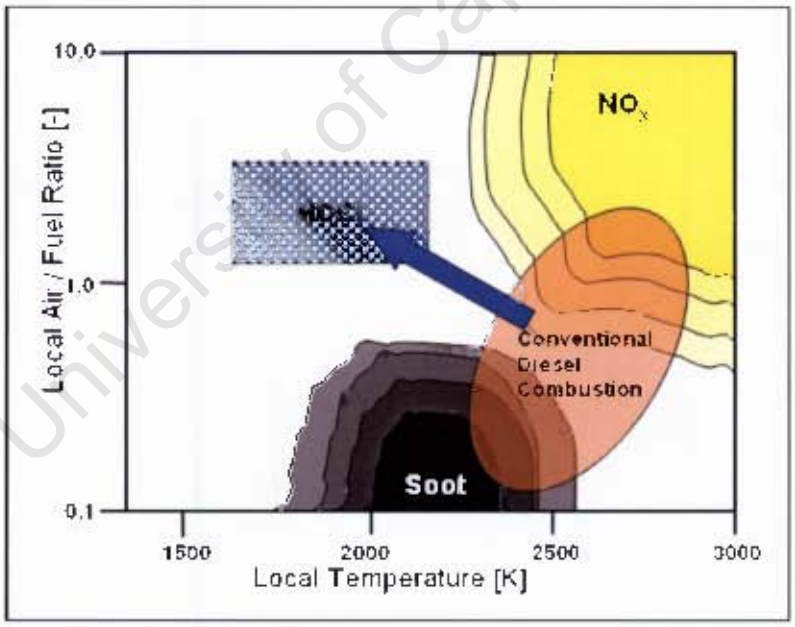

Figure 2-1: Comparison between HCCI and CI engine emissions. Adopted from Velji et al. (2005)

HCCI is potentially applicable to both automobile and heavy truck engines. It could be scaled to virtually every size- class of transportation engines from small motor cycles to large ship engines (U.S. Dep. of Energy, 2001).

2.3 Disadvantages of HCCI

HCCI does pose its own set of unique problems, just like any other IC engine. Some of the disadvantages of HCCI are relatively high hydrocarbon (HC) and carbon monoxide (CO) emissions at low loads, high peak pressures and rates of heat release at high loads, reduced engine speed range and lower maximum power, as well as difficulty in starting the engine and in control of combustion phasing (Milovanovic et al., 2004).

The high levels of HC and CO emissions result from incomplete combustion and quenching effects in crevices in the combustion chamber and near the cylinder wall. The burned gas temperatures are too low to consume the unburned gases during expansion stroke, due to lean burning. Furthermore, the burned gas temperatures are too low to favour the CO to CO2 equilibrium oxidation reaction. All these results in high HC and CO emissions than in SI, where burned gas temperatures are high enough to combust the unburned gases (Stanglmaier et al., 1999, Zhao et al., 2003).

HCCI engine is limited by high rates of heat release at high loads and for this reason, the engine operates lean with high levels of charge dilution being used. This results in lower maximum power output, due to the limited relative air-fuel ratio range. Furthermore, the engine speed range is limited by misfire at high speeds, because there is not enough time for the fuel mixture to autoignite. Figure 2-2 shows the limited HCCI operating range compared to SI engines.

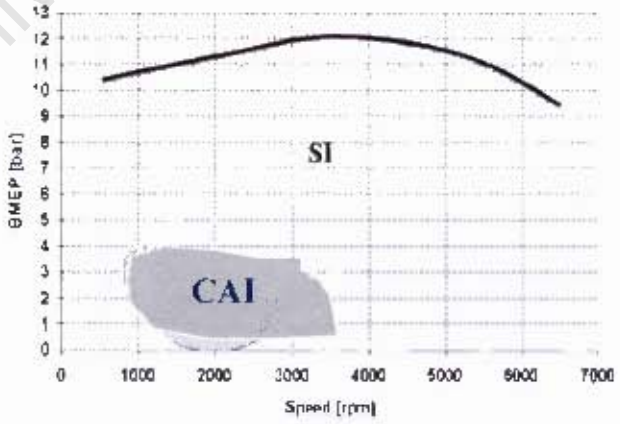

Figure 2-2: Comparison of HCCI (Controlled Autoignition, CAI) and SI load speed operating range. Adopted from Zhao H. (2005)

The greatest challenge facing HCCI engine is the control of combustion phasing over the load and speed range. Since HCCI combustion depends on the ability of the fuel to autoignite by compression, there is no direct control over the start of combustion. The start of combustion is determined by the autoignition chemistry of the fuel mixture, the temperature history and to a lesser extent the pressure history, to mention a few. Therefore, the inlet valve closure (IVC) mixture conditions needs to be precisely controlled in order to obtain optimum autoignition timing (Zhao et al., 2003). However, it is difficult to achieve this level of control during transient engine operation.

2.4 Control Strategies and Operating Range Extension

The major challenge facing HCCI technology lies in maintaining thermal conditions to assure HCCI operation during rapid transient operation. Incorrect thermal conditions and charge composition at the time of autoignition could lead to inevitable misfire or engine knock. Thus, accurate control of thermal boundary conditions is a prerequisite for robust HCCI combustion control over a wide range of engine operating conditions (Zhao et al., 2003).

It is well understood that autoignition of lean fuel-air mixture is dominated by the mixture properties and time-temperature history to which the mixture is exposed. Several approaches have been attempted to control and extend the load and speed operating range of the engine. The approaches are distinguished between those methods attempting to control the time-temperature history to which the mixture is exposed and the methods aimed at altering the propensity for autoignition of the mixture (Stanglmaier et al., 1999). Some of the methods that have been investigated in literature were reviewed to explore their advantages and disadvantages. This review provided understanding of what needed to be done to overcome the present challenges. The methods that have been reviewed are summarised below.

2.4.1 Intake temperature

HCCI autoignition timing is very sensitive to temperature changes. A higher intake temperature advances HCCI combustion but the controllable range is relatively limited and a large penalty in volumetric efficiency accompanies high inlet temperatures. Furthermore,

ignition timing changes with changes in engine speed and load, unless the inlet charge temperature is varied to compensate. However the compensation is generally a slow process, more especially during transient condition due to limited capability of intake heating (Zhao et al., 2003).

2.4.2 Compression Ratio

An increase in compression ratio increases the in-cylinder pressure and temperature under compression and expansion, thus advancing combustion phasing. For this reason, a variable compression ratio (VCR) engine has the potential to achieve satisfactory operation in HCCI mode over a wide range of conditions. This is true because the compression ratio can be adjusted as the operation condition changes (Epping et al., 2002). However, a fast control system that modifies the compression ratio in fractions of a second is required for the fast changing conditions in vehicular application. This approach would add some cost and complexity to the engine. Furthermore, the increased CO emissions due to faster expansion leading to a reduced reaction time limit the application of this technique (Haraldsson et al., 2002).

2.4.3 Exhaust Gas Recirculation (EGR) and Residual Gas

Exhaust gas recirculation is probably the most practical way of controlling charge temperature in HCCI engine. Hot residuals proved to enhance HCCI combustion mainly due to the high temperature of the resulting mixture. Residuals are also used to control the heat release rate due to their impact on chemical reaction rates, which can delay autoignition time. Therefore, reducing the heat release rate results in lower peak cylinder pressures. External EGR works well due to its simplicity, but its thermal effect is limited as a result of heat loss. In addition, external EGR systems have slow response during transient operation.

An alternative approach is to trap exhaust gas residual in the cylinder via variable valve actuation (VVA) or variable valve timing (VVT). According to Haraldsson et al. (2002), internal EGR through VVT eliminates many of the system issues encountered with the external EGR approach. Zhao et al. (2003) found that even with internal EGR the main effect on HCCI combustion is thermal, and that the primary influence of the charge dilution is on the

main combustion. Although, a VVT system adds cost to engine, several manufactures already have VVT systems in production.

Hiraya et al. (2001) found that small amounts of residuals and lower intake temperature reduce the air–fuel ratio operation range of a naturally-aspirated gasoline HCCI engine. In comparison, a large amount of residual and higher intake temperature expand the relative air-fuel ratio range for stable combustion, but with a dramatic reduction in indicated mean effective pressure (IMEP). Furthermore the maximum load and volumetric efficiency were found to decrease with an increase in EGR rate due to combustion deterioration. It was concluded that the load range cannot be extended through residuals for a naturally-aspirated gasoline HCCI engine.

2.4.4 Water Injection

Water injection has been attempted as a control method for delaying the start of combustion and slowing the heat release rate in HCCI engines. Christensen et al. (1999) confirmed the possibility to control ignition timing in a range of operating conditions with the use of water injection, but with the penalty of an increase in HC and CO emissions.

Kaneko and co-workers (2002) found that water injection can reduce heat release rate and possibly extend the operating range of diesel HCCI engine. However, the amount of water injected is limited to the minimum required for sufficient suppression of overly-advanced combustion due to the increase in HC emissions and indicated specific fuel consumption (ISFC).

2.4.5 Forced Induction

Boosting is regarded as an effective way to increase indicated mean effective pressure (IMEP) and extend the operating range of the relative air-fuel ratio for HCCI combustion mode (Zhao et al., 2003). Christensen et al. (1998) has achieved HCCI operation up to 14 bar IMEP, using an externally boosted engine fuelled with methane. However, the resulting high in-cylinder pressures and heat release rates limit the potential of this technique.

2.4.6 Fuel Injection

Direct injection (DI) provides the potential to control HCCI combustion by altering the local fuel concentration via varying the injection timing. It also alters the gas temperature through charge cooling from fuel evaporation. Although DI promises control of HCCI combustion, Takeda et al. (1996) and Nakagome et al. (1997) proved it to be an ineffective method for controlling the combustion phasing of diesel HCCI due to poor vaporisation of diesel fuel. This poor vaporisation of diesel fuel resulted from the charge cooling provided by direct fuel injection.

In gasoline HCCI, controlled fuel stratification through DI can be a potential control parameter for combustion phasing (Marriott et al., 2002a). Injection timing for single and split-injection have been used to provide a homogeneous or stratified fuel charge, but smoke limited the level of fuel stratification. Fuel stratification improved combustion efficiency due to reduced HC emissions, at a price of increased NO_x emissions (Marriott et al., 2002b). Split-injections were reported to be more effective for reducing heat release rate and increasing the overall load and speed range of acceptable stratified combustion (Marriott et al., 2002a).

2.4.7 Dual-Mode Operation

Currently, HCCI operation is limited to part-load operating conditions, because of high heat release rates and pressure rise rates that reduce the benefit of this technology at higher loads. For this reason, it is generally accepted that HCCI will be operated as a dual-mode engine. The engine is operated in HCCI mode at light loads and switched to either SI or CI at high load operating conditions where HCCI benefits are minor and HCCI control is more difficult. Due to cold start difficulties that results from very low temperature and high heat loss from the compressed charge, the engine is stated on conventional SI or CI mode and then switched to HCCI mode a short after warm-up period (Thring, 1989, Ishibashi et al., 1996).

2.4.8 Glow Plugs

Amongst other strategies, glow plugs have been considered as the practical way to obtain effective HCCI control, particularly during cold start. However, their development for practical application is limited especially during rapid transient by their heating capacity, response time and complicated system control.

2.5 Fuel Perspective on HCCI

Although HCCI combustion has been achieved with multi-fuels, fuel selection for HCCI is still an important aspect for this engine development. The main fuels that have been used include gasoline, diesel fuel, propane, natural gas, ethanol, methanol and single and dual component mixtures of gasoline primary reference fuels; PRF (blends of n-heptane and iso-octane). Volatility and autoignition characteristic are identified as the most important parameters of a fuel for HCCI technology.

In dual-mode operation, the fuel must meet both the low load HCCI requirements and the high loads performance criteria. In the case of gasoline HCCI combustion, the fuel must have low octane rating (the ability of the fuel to resist autoignition) to readily autoignite, whereas the fuel has to have high octane rating to sustain the conventional SI engine knock at high loads. For diesel fuel the opposite is true, low cetane fuel is desirable for HCCI combustion, whereas high cetane fuel is desirable at high loads (Zhao et al., 2003).

Some additives have been used to promote or inhibit the heat release rate of autoignition so as to obtain good performance across the speed and load range of the engine. These additives were added to the fuel to make it more chemically reactive or inhibitive, in attempting to control HCCI autoignition. Some additives that advanced combustion by almost 11 crank angle degrees when added to the intake mixture were identified (Aceves et al., 2003, Ogawa et al., 2003). However, the use of some additives is limited by emission legislations and cost of production.

Furutani et al. (1998) proposed an approach that uses dual fuel to enable autoignition timing control. The technique combines the main fuel with high octane number (ON) and a secondary fuel with low octane number. The potential of this procedure has been studied for

a combination of methane and dimethyl ether (DME) (Flowers et al., 2000) and a combination of iso-octane and n-heptane (Olsson et al., 2001). The dual fuel method proved to be effective in combustion phasing control. However, this method would require carrying and refilling two fuel tanks.

An alternative approach is to use one fuel tank with on-board fuel reforming, which is the dissociation of the hydrocarbon fuel into gas components (i.e. CO and H_2). A portion of the fuel would be reformed and used as a secondary fuel. This technique was demonstrated with ethanol fuel and it was found that hydrogen in the reforming products significantly increased chain branching of the system, which improved ignition (Ng and Thomson, 2004). However, NO_x emissions were increased because of the increased peak temperatures due to the energy that was put into the system to reform the fuel.

Given the unique characteristics of gasoline and diesel fuel, a blend of the two fuels could probably the desirable HCCI operation over a wide range of operating condition (Zhao et al., 2003). Nevertheless, further research on how to avoid the dual fuel system is continuing.

2.6 Autoignition of Hydrocarbon Fuels

Tanaka and co workers (2003) conducted a study on the effect of the fuel structure, mixture composition and additives on HCCI combustion. The investigation indicated two-stage ignition for all the saturated compounds and olefins. On the other hand, cyclic unsaturated compounds and some aromatics showed a single-stage ignition. Two-stage ignition is characterised by partial oxidation at low temperatures (referred to as cool flame) followed by a distinct time delay before complete oxidation (referred to as hot flame). In comparison, single-stage ignition is characterised by the induction interval, which is followed by a very rapid reaction rate (hot flame).

In simple terms, single-stage ignition does not exhibit the low temperature reactions (cool flame and NTC), but only high temperature reactions. Figure 2-3 shows the distinct temperature regimes observed in two-stage ignition and figure 2-4 shows the difference between fuels with single-stage ignition and two-stage ignition at 40 bar. These figures show ignition delays obtained from Chemkin modelling of n-heptane and toluene. The pressure

effect of reducing ignition delay as it is increased is more pronounced in the intermediate and high temperature regime.

Edward et al. (1992) identified the temperature range below 700 K as "low", from 700 – 1100 K as being "intermediate", and > 1100 K as "high" temperature regime. More recently however, most workers in the field of detailed kinetics of hydrocarbon oxidation, prefer not to distinguish a separate low temperature regime, but rather to identify the range from 600 – 900 K as the low-intermediate regime (Tao et al., 2002).

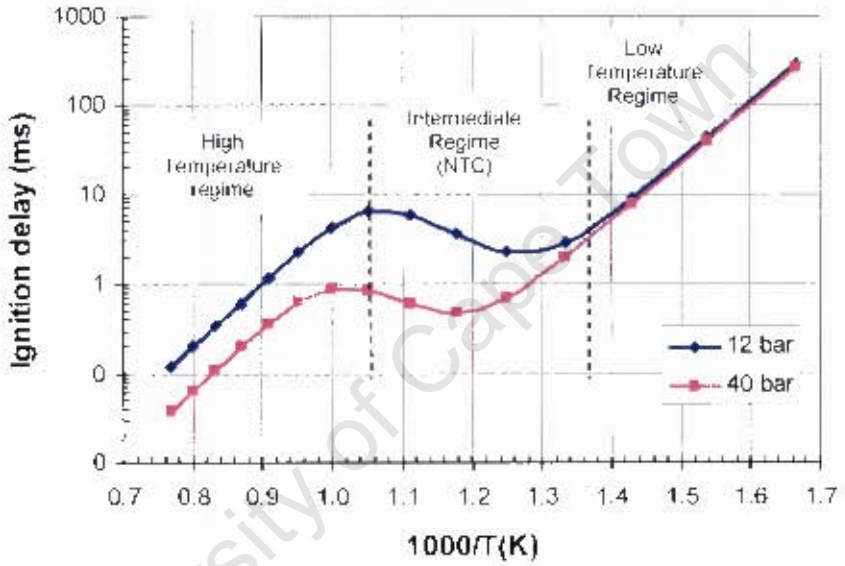

Figure 2-3: Different temperature regimes observed in two-stage ignition of hydrocarbon fuel

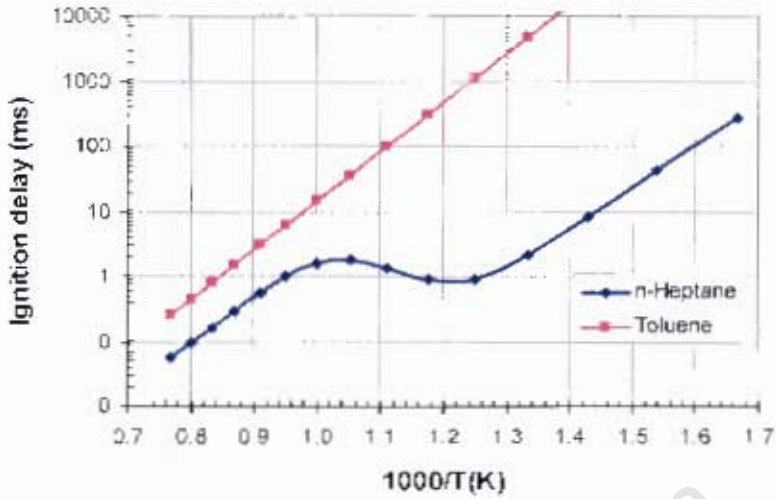

Figure 2-4: Difference between fuels with single-stage ignition (Toluene) and two-stage ignition (n-Heptane) at 26 bar

This behaviour of hydrocarbon fuels have been obtained by different researchers and it well understood that some hydrocarbon fuels exhibit two-stage ignition, whereas some single-stage ignition (Cox et al., 1985, Rifkin and Walcutt, 1957). Leppard (1990) concluded that the negative temperature coefficient (NTC) behaviour of a fuel tends to retard autoignition of a fuel relative to one that does not exhibit such behaviour.

2.7 *Autoignition Models*

Different types of models for autoignition have been developed, ranging from a complete global, single step description (Warnatz, 2000), to a reduced kinetic treatment (Halstead et al., 1977, Cox et al., 1985, Griffiths et al., 1994), or a comprehensive, detailed chemical kinetic simulation (Westbrook et al , 1988). The models are classified in to two categories: 1) Chemical kinetic mechanisms, and 2) Empirical ignition delay correlations.

2.7.1 Chemical Kinetic Mechanisms

Detailed chemical kinetic mechanisms have been developed to predict autoignition and bulk burn rates across all operating conditions and to determine the critical reaction pathways. The mechanisms for fuels incorporate hundreds of species and thousands of reactions, for

example the mechanism for n-heptane consists of 2750 elementary reactions and 550 species (Curran et al., 1998). These mechanisms model the two-stage cool flame ignition and the subsequent hot ignition very well. Although detailed mechanisms for different fuel components are developed, no detailed mechanisms are yet available for use with real blended fuels in engine. Moreover, detailed kinetic mechanisms are complex and require longer computational time.

Although detailed mechanisms provide the opportunity to model combustion systems over a wide range, the problem is that they are too computationally intensive for most applications. Therefore, reduced mechanisms were derived from the detailed mechanisms to offer the possibility of the pragmatic deduction of blending rules amongst different classes of compounds. Reduced mechanisms fail to describe in satisfactory manner the transition to high temperature reactions, above approximately 1200 K (Griffiths, 1995). Moreover, the parameters of the reduced model cannot be predicted from first principles and the model itself is inevitably dependent on empirical data for calibration (Viljoen et al., 2005).

2.7.2 Empirical Ignition Delay Correlations

Single-step mechanisms include no elementary chemical kinetic information, but attempts to represent the sum of all the hydrocarbon oxidation reactions with a single, global reaction approach. A single Arrhenius equation was used, with a rate constant k of:

$$k = Ae^{\left(\frac{-E_a}{RT}\right)} \qquad (2\text{-}1)$$

Where A is the pre-exponential constant of proportionality

E_a is the activation energy

R is the universal gas constant

Livengood and Wu (1955) developed a simple conservation-of–ignition delay concept to correlate autoignition times (ignition delay) from a rapid compression machine (RCM) to those measured in SI engines. Ignition delay (τ) correlation included possible pressure dependence, in the form:

$$\tau = Ap^{-n}e^{\left(\frac{B}{T}\right)} \tag{2-2}$$

Where A, n, and B are empirical constants that are calibrated from experimental data. A is the proportionality constant, n is the pressure coefficient and B is the temperature coefficient.

In simple terms, ignition delay is the time delay from injection of fuel to the onset of autoignition. Since RCM operation assumes constant pressure, an integral of the inverse of the ignition delay was used to allow for the time-variant pressure and temperature in a running engine. It was assumed that autoignition occurs when the integral attains a value of one.

$$\int_{t_0}^{t_c} \frac{dt}{\tau} = 1 \tag{2-3}$$

Where t_0 is the starting time, and t_c is the time at ignition.

The same approach was used by Douaud and Eyzat (1978) to correlate autoignition in SI engines over a range of operating conditions using different fuels with different octane ratings. An ignition delay correlation for primary reference fuels (PRF) was proposed, in the form:

$$\tau = 0.01869\left(\frac{ON}{100}\right)^{3.4017} p^{-1.7} e^{\left(\frac{3800}{T}\right)} \tag{2-4}$$

Where ON is the octane number of the fuel.

The scope of the model was limited to the range covered by the calibration 80 ≤ ON ≤ 100. Since the model is a single-step correlation that attempts to represent the ignition delay of three distinct regimes, the NTC behaviour of some hydrocarbon fuels could not be observed. Figure 2-5 and 2-6 show that it is more likely to describe the average of the three ignition delays.

Most recently, Yates and co-workers (2004) proposed a 3-part Exponential model so as to account for the NTC behaviour of some fuels. The model involved two distinct regimes, a two-stage low temperature regime and a single-stage high temperature regime. The ignition delay for each regime was described by equation 2-2. The stages of the low temperature regime were sequential and were expressed as an arithmetic sum of the individual ignition delays, $\tau_1 + \tau_2$. The high temperature regime represented an alternative competing pathway with an ignition delay of τ_3. The total ignition delay for the full temperature and pressure range was described by the inverse sum of the two options:

$$\tau_{overall} = \left\{ \left(\tau_1 + \tau_2\right)^{-1} - \left(\tau_3\right)^{-1} \right\}^{-1} \qquad (2\text{-}5)$$

This model provides enormous improvement over the Douaud and Eyzat model, since it accounts for the NTC behaviour of some fuels. Figures 2-5 and 2-6 show the differences between the 3-part Exponential model and Douaud and Eyzat model at 12 and 40 bar, respectively. However, the application of the model is limited to the available fuel data for the calibration of the nine coefficients.

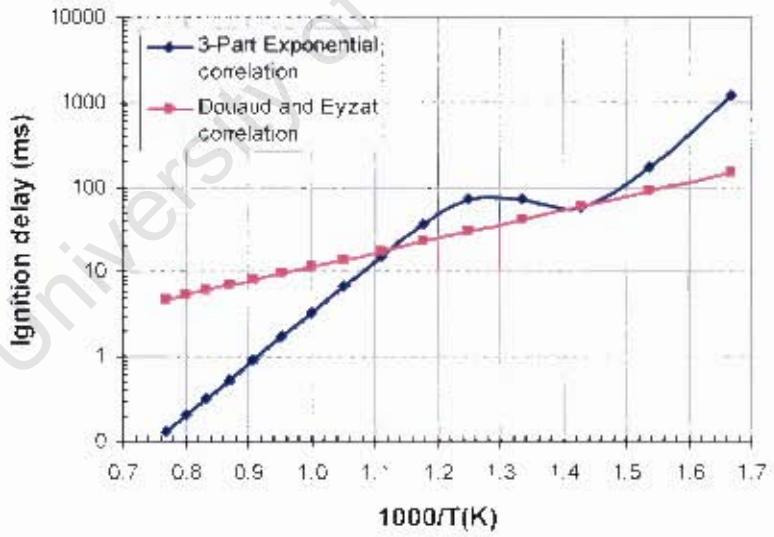

Figure 2-5: Comparison between the 3-part Exponential model and Douaud and Eyzat model at 12 bar for Iso-octane

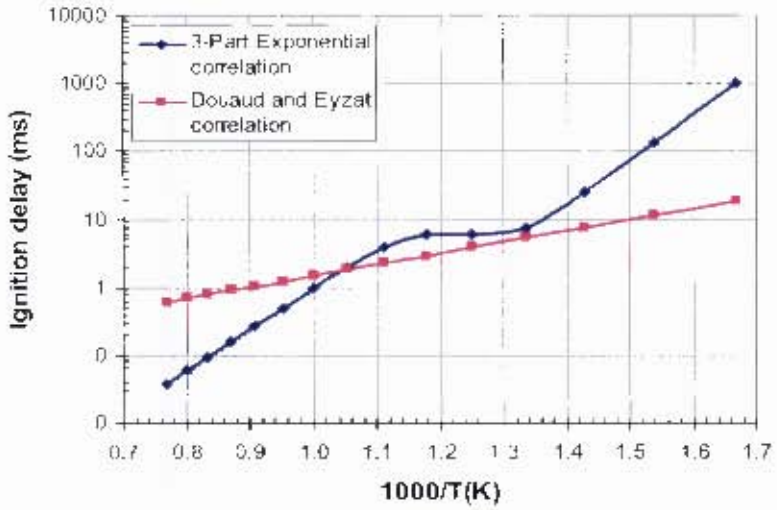

Figure 2-6: Comparison between the 3-part Arrhenius model and Douaud and Eyzat model at 40 bar for iso-octane

All these models were originally developed to predict autoignition of the end gas in conventional SI engines under stoichiometric conditions. This means that the available calibrated values for the empirical constants for different fuels were obtained at a relative air-fuel ratio of one.

2.8 Heat Release Rate and Combustion Duration

The Wiebe function is probably the most commonly used functional representation of the mass fraction burnt in the flame propagation of SI engine. It describes the shape of the mass fraction burnt by the appropriate choice of parameters:

$$x_b = 1 - \exp\left[-a\left(\frac{\theta - \theta_0}{\Delta\theta}\right)^{n+1}\right] \qquad (2\text{-}6)$$

Where θ is an instantaneous crank angle

θ_0 is the start of main heat release (SOC)

$\Delta\theta$ is the combustion duration

The parameters, a, and b, are used as descriptors for the burn rate of the fuel. A smaller multiplier, a, for example, is indicative of a later pressure rise, whilst a smaller exponent, b, shows an earlier pressure rise (Swarts et al., 2004).

A number of researchers used the Wiebe function to describe the shape of heat release in HCCI combustion modelling (Erlandsson et al., 2002 and Roelle et al., 2004).

In most cases, the burn duration is obtained from chemical kinetics and is taken from the crank angle of 10% heat release (CA10) to the crack angle of 90% heat release (CA90). The duration for HCCI combustion was found to be dependent on inlet mixture composition, amount exhaust gas recirculation, temperature of unburned mixture and cylinder pressure as well as engine speed (Noel et al., 2004, Kontarakis et al., 2000, Peng et al., 2003, Babajimopoulos et al., 2002). Moreover, it was found to be significantly shorter than in SI engines, and varies between 3 to 20 crank angle degrees, depending on the operating conditions.

Very little work has been done in developing HCCI combustion duration correlations over a wide range of operating conditions. Some researchers assumed constant burn duration in their studies (Roelle et al., 2004). Kawanabe et al., (2004) developed an empirical correlation to predict HCCI combustion duration based on the conditions at the start of main combustion event. The combustion duration was defined as the period from 5% to 95% temperature increase, and is of the form:

$$1/\tau_{cd} = 6.1\times10^{31}(Md)^{0.52}F^{3.2}O^{26.5}\exp(-12500/T_u) \qquad (2\text{-}7)$$

Where τ_{cd} is the combustion duration (ms)

Md is the molecular density of the mixture

F, O are the fuel and oxygen mole fractions, respectively

T_u is the temperature of the unburned gases

This combustion duration correlation does not give any information on the development, but only gives the total combustion duration.

3 Combustion Modelling

This chapter discusses combustion and ignition delay modelling as well as the theoretical setup and how all these were integrated to obtain the desired ideal fuel.

3.1 Engine Model

This study employed a two-zone, pseudo-dimensional thermodynamic engine cycle model. The model represented the chamber attributes of the Ricardo E6 engine so that it could be calibrated against the experimental results from a parallel HCCI study. The key parameters of the engine are shown in table 3-1. The model was based on the following assumptions:

- Uniform pressure
- Infinitely thin wall separating the two zones
- Zero heat transfer between the zones
- Blow-by and crevices were ignored
- Fuel was completely evaporated and well mixed
- Heat transfer by convection only and radiation neglected, and
- A compositionally frozen unburnt zone

The temperatures of the two zones were calculated from the conservation of energy, allowing for combustion reactions, piston work and heat losses. The convection coefficient h_{conv} from the Woschni correlation discussed in Stone (1999) was adopted for in-cylinder, intake and exhaust manifold heat transfer, of the form:

$$h_{conv} = 129.8 B^{-0.2} p^{0.8} T^{-0.55} \left(C_1 \bar{S}_p + C_2 \frac{V_d T_{IVC}}{p_{IVC} V_{IVC}} (p - p_m) \right)^{0.8} \qquad (3\text{-}1)$$

Where B is the cylinder bore, p is the instantaneous cylinder pressure, T is the instantaneous gas temperature, S_p is the mean piston speed, V_d is the displaced volume, p_{IVC}, V_{IVC}, T_{IVC}, are the working-fluid pressure, volume and temperature at inlet valve closure (IVC) and p_m is the motored cylinder pressure at the same crank angle as p.

The scalar C_1 is 6.18 for gas exchange, otherwise 2.28 and the scalar C_2 is 3.24 x 10^{-3} for combustion and expansion, otherwise 0.

Parameter	Value and units
Bore	76.2 mm
Stroke	111.1 mm
Conrod/Crank radius	4.3
Displaced volume	506.8 cc
Maximum Valve Lift	8.5 mm
IVO	9° BTDC
IVC	36° ABDC
EVO	42° BBDC
EVC	8° ATDC

Table 3-1: Engine Specifications

The composition of the burnt zone was calculated from the carbon, hydrogen and oxygen balances, as well as equilibrium dissociation and water gas shift reactions. Thermodynamic properties were obtained from polynomial regression curves fitted to the JANAF thermodynamic tables.

The trapped mass temperature and pressure at inlet valve closure (IVC) were calculated from the breathing model. The breathing model would start by exhausting (Exhaust Valve Opening, EVO) the waste gases from the previous cycle and drawing in fresh charge up to the inlet valve closure (IVC). Before the model could run, the user had to specify the following input parameters: engine speed (N, rpm); intake manifold pressure (P bar); intake manifold temperature (T, K); fuel in used from the fuel blending model; compression ratio (CR); fuel-air equivalence ratio (Φ) and exhaust gas recirculation (EGR, mass %). It incorporated an ideal mixing of the fresh charge and the specified external residual fraction which comprised of the products of combustion (either stoichiometric or non-stoichiometric). A flow diagram illustrating the operation of the engine cycle model is given in figure A-2 of Appendix A.

Trapped residuals were estimated to be at most 5% by mass, and their effect on the results was assumed to be negligible. The breathing model was designed to incorporate friction and entry losses in the manifold, as well as the effect of backflow and valve overlap. Furthermore, it was assumed that all the fuel in the trapped cylinder mass was evaporated at the time of IVC. This was a necessary prerequisite for the application of the ideal gas law during the engine cycle. More details on the engine model are provided in Appendix A.

3.2 Ignition Delay Model

The selection of the ignition delay model used with the engine model was based on cost and computational time. The decision was taken to use the three part Exponential model coupled with the conservation of ignition delay model of autoignition to predict combustion phasing (see equations 3-2 to 3-4). Since the nine parameters (A_i, B_i and n_i) characterising each fuel were all developed for stoichiometric mixtures, the overall ignition delay was corrected for relative air-fuel ratio and exhaust gas recirculation. These corrections were necessary since HCCI engine operates very lean and uses large amounts of charge dilution.

$$\tau_i = A_i p^{n_i} e^{\frac{B_i}{T}} \tag{3-2}$$

$$\tau_{overall} = \{(\tau_1 + \tau_2)^{-1} + (\tau_3)^{-1}\}^{-1} \tag{3-3}$$

$$\int_0^{t_c} \frac{dt}{\tau_{overall}} = 1 \tag{3-4}$$

Chemical reaction schemes for primary reference fuels (PRF) used to define the Octane Scale were used to cover the octane spectrum. The differential equations describing the reactions were solved using Chemkin Collection (Version 3.7) over a wide range of pressure of 12 and 40 bar. Autoignition of the fuel was signalled by an exponential increase in the temperature and the ignition delay (in milliseconds) was defined by the time that had elapsed until a temperature threshold of 1400 K was reached. The development of the correlations is summarised in the following sections and more details are listed in Appendix B.

3.2.1 Relative air-fuel ratio Correction

The relative air-fuel ratio (λ) effect on ignition delay was studied by varying the fuel-air equivalence ratio (Φ) from 0.2 to 4. Ignition delay for a range of PRF starting from 0 to 100 research octane number (RON) were obtained from Chemkin for each fuel air equivalence ratio. An excellent correlation was obtained by fitting the Chemkin results to a simple power law, of the form:

$$\tau_{corr} = \tau_{\lambda=1}\lambda^{k} \quad (3\text{-}5)$$

Where $\tau_{\lambda=1}$ is ignition delay at stoichiometric conditions, given by equation 3-3 and τ_{corr} is the corrected ignition delay (in milliseconds) at a given relative air-fuel ratio. The constant k was obtained to be 0.775 for the selected pressure range and was independent of fuel octane rating. This value of k was used throughout this study. More details on the development of this correlation are given in Appendix B.

3.2.2 Exhaust Gas Recirculation Correction

Exhaust gas recirculation (EGR) was varied for 0 to 50% on mass basis and ignition delay for three PRF (0, 50 and 90) at each step were obtained using Chemkin. Unfortunately, a simple correlation could not be obtained due to the fact that EGR changed the trapped mass composition. However, it was possible to extend equation 3-5 to incorporate the effect of EGR and the resulting correlation was of the form:

$$\tau_{o,corr} = \tau_{\lambda=1}\lambda^{k}\left(1-\frac{\%EGR}{100}\right)^{m} \quad (3\text{-}6)$$

Where $\tau_{o,corr}$ is the corrected overall ignition delay, %EGR is the percentage of EGR (by mass) and the value of m was found to be dependent on the inlet fuel-air equivalence ratio. For the conditions already discussed above, the dependence was of the parabolic form (equation 3-7), with the constants adjusted to fit Chemkin results. Furthermore, these constants are independent of fuel octane number and were used through out this study. Further details on the development of this correlation are given in Appendix B.

$$m = -0.615\phi^{2} + 0.0521\phi - 0.0323 \quad (3\text{-}7)$$

3.3 HCCI Engine Model

HCCI combustion was modelled using the engine model coupled with the ignition delay model. The ignition delay model was incorporated according to the flow diagram given in figure A-1 of Appendix A. Although the ignition delay model included the low temperature ignition delay, the heat release during the low temperature oxidation was excluded. Therefore, the model predicted the start of main heat release based on the compression pressures and temperatures. At this point, the combustion duration was predicted with equation 2-7 using top dead centre (TDC) conditions of the motored engine.

Ignition delay data of the fuel was required before the ignition delay model could be applied. For this reason, ignition delay characteristics of fuels were obtained from Chemkin using chemical reaction schemes for specific fuel species that were considered to represent the main broad classification of hydrocarbon species. Table 3-2 shows the different classes of the fuel components and their research and motor octane number (RON and MON, respectively). The details on how the fuels were characterised were discussed by Yates et al. (2005).

Fuel	Generic Classification	RON	MON
N-Heptane	Linear paraffins	0	0
Iso-Octane	Iso-paraffins	100	100
1-Hexene	Olefins	76.4	63.4
Toluene	Aromatics	120	109
Methanol	Oxygenates	106	92

Table 3-2: Classification of known fuel components and their octane numbers (ON)

3.3.1 Burn Rate and Duration

In this study, the burn rate of the fuel was assumed to conform to the Wiebe function already discussed in chapter 2. The parameters, a, and b, were assigned the values used in Heywood (1988) of 5 and 2, respectively. The start of main heat release (SOC) was predicted using the ignition delay mathematical model discussed previously.

The burn duration correlation developed by Kawanabe et al. (2004) was adopted to predict the combustion duration based on the conditions at the start of main combustion event. The

duration obtained from this correlation was expressed in crank angle degrees (Δθ) using the engine speed effect and then used in the Wiebe function to model heat release rate.

3.3.2 Engine Model Performance and Efficiencies

The engine performance at each operating condition was measured by the indicated mean effective pressure (IMEP), which is the amount of work done per engine cycle. IMEP was defined as

$$IMEP = \frac{W_c}{V_d} \tag{3-8}$$

Where W_c is the engine work done per cycle, and V_d is the engine displacement volume.

A friction model was incorporated in the engine model from Stone (1999) and was extended to account for compressor and intercooler losses during forced induction. The friction model was extended to include the effect of forced induction on mechanical efficiency. Pumping losses were assumed to be negligible. Friction mean effective pressure (fMEP) was calculated as follows:

$$fMEP = 0.061 + \frac{p_{\max}}{60} + 2.29 \times 10^{-4} N + \frac{W_{comp} + Q_{\text{int}}}{V_d} \tag{3-9}$$

Where P_{max} is the maximum in-cylinder pressure (bar); N is the engine speed (rpm); W_{comp} is the compressor work (J); Q_{int} heat loss in the intercooler (J) and V_d is the engine displacement volume.

The brake mean effective pressure (bMEP) and the mechanical efficiency (η_{mech}) were calculated as follows:

$$bMEP = IMEP - fMEP \tag{3-10}$$

$$\eta_{mech} = \frac{bMEP}{IMEP} \tag{3-11}$$

The indicated thermal efficiency (η_{th}) was calculated from the equation obtained in Heywood (1988) with the combustion efficiency (η_{comb}) assumed to be 100%.

$$\eta_{th} = \frac{W_c}{m_f Q_{LHV} \eta_{comb}} \tag{3-12}$$

Where W_c is the work done per cycle; m_f is the mass of fuel inducted per cycle and Q_{LHV} is the low heating value of fuel.

For the purpose of investigating the operating range of HCCI, the engine was assumed to be knocking if the rate of pressure rise (dP/dθ) exceeded 10 bar per crank angle degree (Aroonsrisopon et al., 2002). Knock limit was set as:

$$\frac{dP}{d\theta} \leq 10 \tag{3-13}$$

3.4 Theoretical Approach

This section discusses the approach taken in producing the results and describes the setup for each test performed in this study.

3.4.1 Model Validation

The first step before proceeding to the design of fuel was to test if the model performed as expected. The engine test conditions are shown in table 3-3. The engine was operated in HCCI mode at different compression ratio ranging from 7.5:1 to 14:1 and relative air-fuel ratios (λ) ranging from 2 to 4. All the other inlet parameters were kept constant as given in the tables below and the fuel used in the test was n-heptane. All the experimental results used to validate the model were obtained from a parallel HCCI study by Rabe (2006).

Parameter	Value and units
Engine Speed	1000 rpm
Intake Manifold Pressure	1 bar
Intake Manifold Temperature	340 K
Relative air-fuel ratio (λ)	2 – 4
Compression ratio	7.5:1 – 14:1
Exhaust gas recirculation (EGR)	0 %
Fuel	n-Heptane

Table 3-3: Engine Test condition for model validation

At each test condition the experiment was repeated 3 times for repeatability of results. These experimental results were compared with the model results at the same conditions. The pressure profiles from both the experiment and model were recorded for comparison. At this stage there were no adjustments made on all the equations used in the model. The parameters of the Wiebe function for modelling heat release were standard from Heywood (1988) as were the Woschni equation parameters for heat loss from Stone (1999).

3.4.2 Known Fuel Combustion Analysis

The next step after gaining confidence on the ability of the model to predict the start of combustion and heat release rate was to use it to study combustion of known fuels in details. The fuels used in this study are given in table 3-2 and the information of their detailed chemical kinetic reactions is given by Viljoen et al. (2005). The ideal was to cover the whole octane range and verify the octane effect on HCCI combustion as well as obtaining the idea of the fuel required for this type of engine. The test fuels autoignition characteristics and ignition delay curves are given in Appendix C.

It has been concluded that the chemistry of real fuels containing aromatics, olefins and alcohols is different from that of paraffins and that such fuels are sensitive (Kalghatgi, 2003 & Risberg et al., 2003). With regard to this conclusion, the effect of fuel sensitivity was also investigated. Fuel sensitivity was defined by the equation of the form (Kalghatgi, 2003):

$$Fuel\ Sensitivity = RON - MON \qquad (3\text{-}14)$$

Where RON is the research octane number of the fuel component and MON is the motor octane number of the fuel component.

These different fuel components had different properties and ignition delay characteristics that posed difficulties in comparison of the results. In order to overcome the difficulties, optimum inlet conditions were selected for the test to ensure that combustion occurs within 10 CAD of TDC with each test fuel. The model was then run for each fuel at these conditions (see Table 3-4) and the required results have been obtained for comparison.

Parameter	Value and units
Inlet Pressure	1 bar
Inlet Temperature	390 K, 410 K
Relative air-fuel ratio (λ)	4, 2
Compression ratio	18:1, 15:1
Exhaust gas recirculation (EGR)	0 %
Engine speed	1000 rpm
Fuel	Varied

Table 3-4: Engine model conditions for the test on different known fuels

It was not possible to autoignite all the fuels throughout the speed range due to their different requirements of inlet conditions that would enable autoignition. Therefore, n-heptane was selected for further study into the barriers that had to be overcome for operating in the full range. The selection was based on the propensity of the fuel to autoignite throughout the entire operating range. Intake manifold conditions in table 3-5 were selected to allow autoignition at all operating points. The independent variables in the test were: fuel-air equivalence ratio (ϕ) which was varied from 0.2 to 0.9; EGR which was varied from 0 to 50 % by mass and engine speed which was varied from 1000 to 5000 rpm. The model results including the performances parameters (i.e. IMEP, mechanical and indicated thermal efficiencies) were recorded for each change of the inlet conditions.

Parameter	Value and units
Inlet Pressure	Dependent
Inlet Temperature	340 K
Fuel-Air equivalence ratio (Φ)	Varied
Compression ratio	17:1
Exhaust gas recirculation (EGR)	Varied
Engine speed	Varied
Fuel	N-Heptane

Table 3-5: Inlet conditions for generating load map for n-heptane

It was difficult to achieve n-heptane combustion at high speeds, because the engine cycle time was short and the fuel ignition delay was long. It was also difficult to combust the mixture at low equivalence ratios and high EGR rates, because the resulting in-cylinder equivalence ratios were very low for autoignition to occur. These findings were in good agreement with literature (Noel et al., 2004, Yamasaki et al., 2000). For these reasons, forced induction was used to aid autoignition where the mixture could not be ignited naturally.

The intake pressure was varied via the boost pressure, as a dependent variable on engine speed and in-cylinder fuel-air equivalence ratio. The boost pressure was assumed to be provided by a supercharger with compressor efficiency of 90% and an intercooler with the efficiency (η_{int}) calculated from the equation of the form:

$$\eta_{\text{int}} = \frac{T_{in} - T_{out}}{T_{in} - T_{ambient}} \tag{3-15}$$

Where T_{in} is the temperature at the inlet of the intercooler; T_{out} is the temperature at the outlet of the intercooler and $T_{ambient}$ is the ambient temperature (Forst, 2005).

The in-cylinder fuel-air equivalence ratio was determined from the inlet fuel-air equivalence ratio and the amount of exhaust gas recirculation used. Based on the amount of boost pressure required to achieve n-heptane autoignition for given inlet conditions, boost pressure (bar) was correlated to the engine speed (N, rpm) and the in-cylinder equivalence ratio (Φ_{cyl}) with the equation of the form:

$$boost = 2.75 \times 10^{-4} N - 1.5\phi_{cyl} + 0.25 \tag{3-16}$$

Figure 3-1 shows the required amount of boost pressure at a given speed and fuel-air equivalence ratio. This correlation was developed specifically for HCCI combustion with n-heptane fuel.

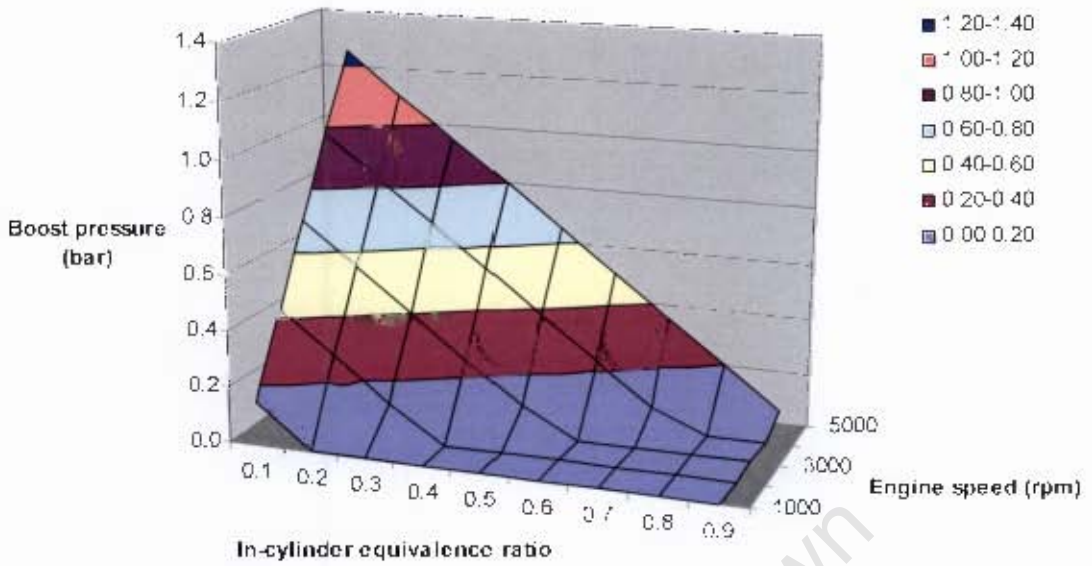

Figure 3-1: Effect of in-cylinder equivalence ratio and speed on boost pressure

The results of the n-heptane test were analysed to obtain the combination of inlet conditions that gave the best performance of the engine model, for a given engine speed. To simplify the analysis procedure, four load points (25%, 50%, 75% and 100% load) were selected based on the maximum attainable IMEP by the engine model, if it was operated as spark ignition (SI) engine[1]. At each load point and speed various combinations of EGR and equivalence ratio were obtained as well as the corresponding mechanical efficiencies. The load map of n-heptane fuel was then produced from the results of the load points.

3.4.3 Fuel Design Method

The challenge was to design a fuel based on the ignition delay characteristic requirements for stable HCCI combustion in the entire operating range. Each fuel can be characterised by three exponential equations, each with three parameters and nine in total. The goal would be achieved if the nine parameters (A_i, B_i and n_i) that characterise the ignition behaviour of the fuel are obtained.

[1] The maximum mean effective pressure for the given speed range was obtained by running the model in SI mode at maximum brake torque (MBT) timing.

In order to solve for the nine parameters, it was necessary to setup nine parametric equations. The equations were established by changing some inlet condition that would cover the desired operating range. The major parameters were identified as fuel-air equivalence ratio, speed and compression ratio. Nine points were selected to cover the whole operating range, three at each load level low, mid and high. The points were as follows: fuel-air equivalence ratio of 0.2, 0.55 and 0.9 representing the load levels, respectively and three speeds (1000, 3000 and 5000) at each equivalence ratio used. The other inlet conditions were kept constant at 1 bar inlet pressure; 0% EGR and 340 K.

The engine model was run according to the flow diagram in figure 3-2 to obtain the required pressure and temperature data. Equations 3-4 and 3-6 were used with the calculated pressure and temperature data to calculate ignition delay and SOC point, respectively. An iterative process was used to solve for the correct parameters that would ensure SOC within 10 crank angle degrees of TDC. The procedure was repeated with different starting parameters until the smallest error was obtained and the resulting parameters would represent the ignition delay characteristic behaviour of the desired fuel.

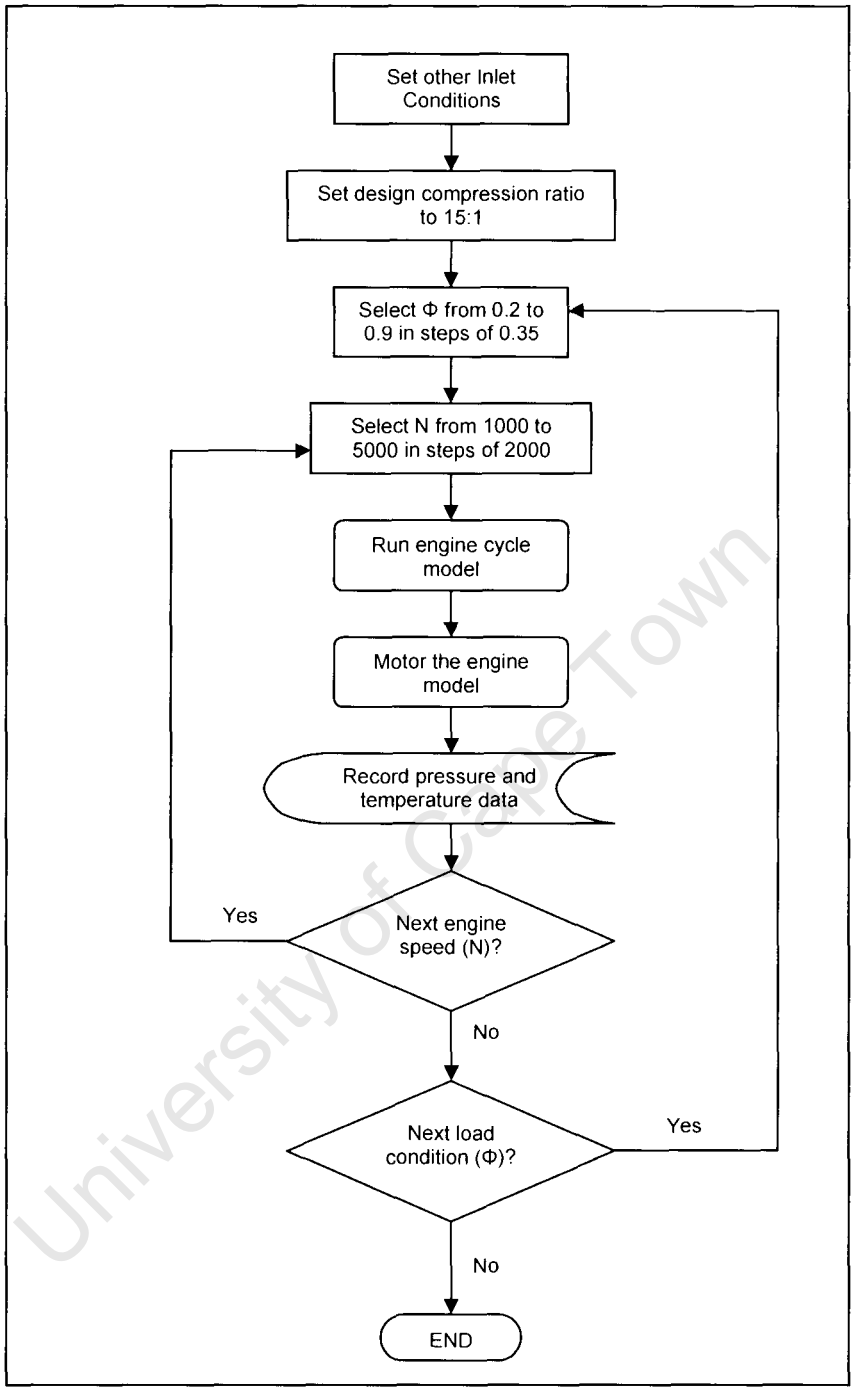

Figure 3-2: Flow diagram for the calculation of the pressure and temperature at the nine operating conditions for the design of the fuel

4 Results and Analysis

4.1 Model validation

The most important aim in this validation was to ensure that the model predicts the combustion phasing and heat release rate (HRR) within reasonable accuracy. The experimental results used to validate the model were obtained from an experimental study on the Ricardo E6 operated in HCCI mode (Rabe, 2006). At each test condition the experiment was repeated 3 times for repeatability of results. The experimental pressure traces for each cycle (P_{cycle}) were recorded for comparison with the model pressure trace (P_{model}) at the same conditions as discussed in section 3.4.1. The comparison of the model and experimental results are shown in the following figures 4-1 to 4-5.

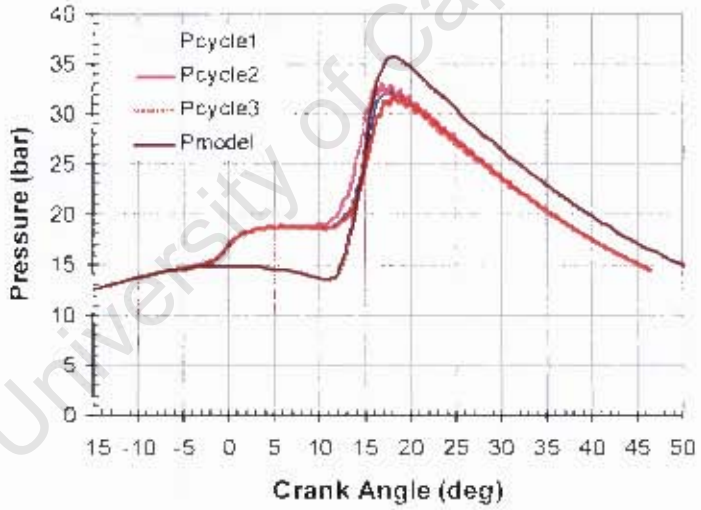

Figure 4-1: Pressure trace at λ = 2 and CR 7.65:1

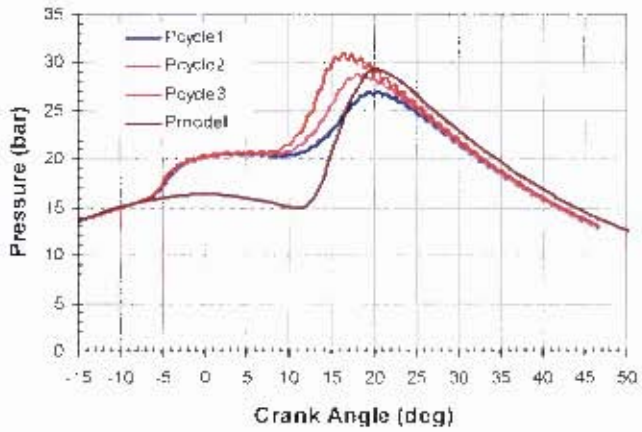

Figure 4-2: Pressure trace at λ = 2.5 and CR 8.14:1

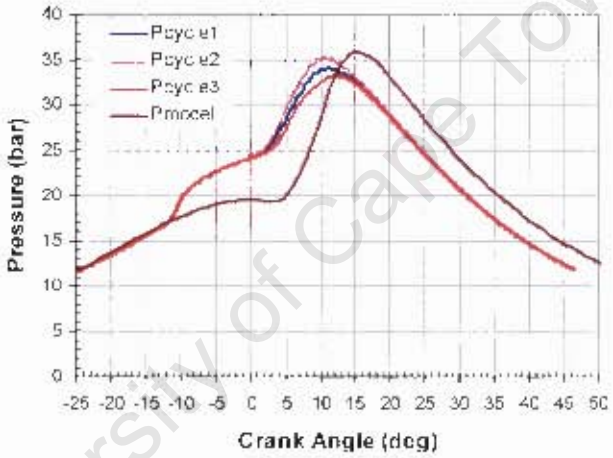

Figure 4-3: Pressure trace at λ = 3 and CR 9.2:1

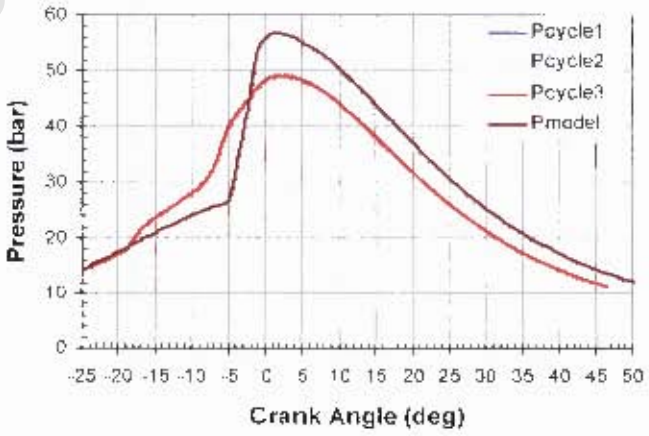

Figure 4-4: Pressure trace at λ = 3.5 and CR 11.8:1

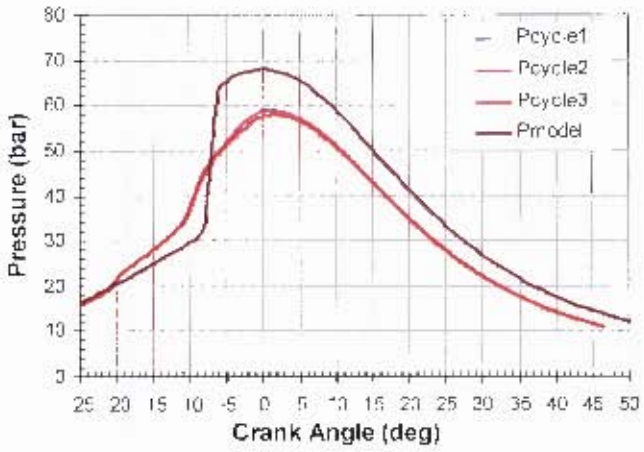

Figure 4-5: Pressure trace at λ = 4 and CR 14.0:1

The first observed difference in the pressure traces was the absence of the first stage pressure rise in the predicted pressure profile. This first stage pressure rise was attributed to the heat released during the low temperature oxidation, which was excluded in the model. Despite the exclusion of low temperature oxidation heat release, the model predicted the start of the main heat release within reasonable accuracy. The second observation was that the predicted start of combustion (SOC) became retarded as the mixture leaned out. This may be associated with the over prediction of heat loss during compression by the Woschni correlation at very lean mixtures.

It can be seen from the above figures that the model over predicts the cylinder pressures during and after combustion. This over prediction occurs during the combustion event and maybe associated with the assumption of complete homogeneity, which is not necessary true for real engine. However, the position of the peak cylinder pressure correlates well with the experiment results. Furthermore, the actual combustion duration becomes longer than the predicted burn duration as the mixture is leaned out. This shorter burn duration results in higher peak cylinder pressures than expected for a lean mixture.

Fiveland et al. (2000) concluded that the Woschni correlation over predicts heat transfer losses and can results in combustion phasing being shifted by 10 CAD. Chang et al. (2004) suggested a new heat transfer correlation for HCCI engines, which was basically an improved Woschni correlation for HCCI engine. The major adjustments were made on the temperature exponent, changed from -0.55 to -0.73 and the unsteady gas velocity term

coefficient was reduced to a sixth of the original value. The improvements on the heat transfer correlation improved the predictions of combustion phasing even for very lean mixtures. The improved Woschni correlation was adopted and the burn duration correlation was fine tuned to ensure better agreement with the experimental results.

Finally, it was noticed from Figures 4-4 and 4-5 that the relative air-fuel ratio effect on the burn duration correlation was dominated by the pressure and temperature effect at high compression operation. The actual burn duration is longer than the model combustion duration due to inhomogeniety in real engines. For this reason, the burn duration correlation was multiplied by a scalar that was linearly dependent to the relative air-fuel ratio. This was done to improve the relative air-fuel ratio effect in the burn duration correlation. The comparison of the improved model results and the experimental results are shown in Figures 4-6 and 4-7 below.

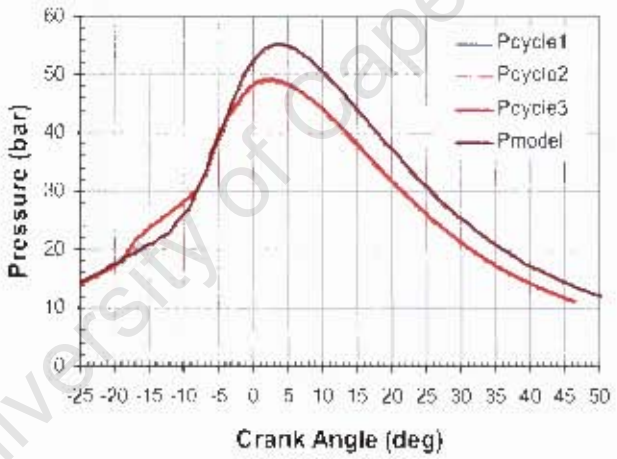

Figure 4-6: Pressure trace at λ = 3.5 and CR 11.8:1, with modified Woschni and burn duration correlations

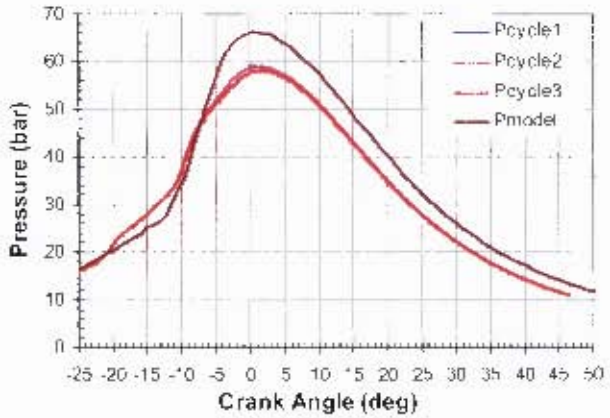

Figure 4-7: Pressure trace at λ = 4 and CR 14.0:1, with modified Woschni and burn duration correlations

An extra model prediction was carried out with methanol as fuel at these inlet conditions: 1 bar inlet pressure; 390 K inlet temperature; relative air-fuel ratio (λ) of 4; 19.55:1 compression ratio and 1000 rpm engine speed with 0% EGR. It included all the improvements that were made in the Woschni and burn duration correlations. Methanol has a single-stage ignition (i.e. does not exhibit NTC behaviour), whereas n-heptane has two-stage ignition. Thus, for methanol the main heat release is the same as the start of combustion. This was important in addressing the concerns about n-heptane predictions. Figure 4-8 shows the comparison of the methanol results.

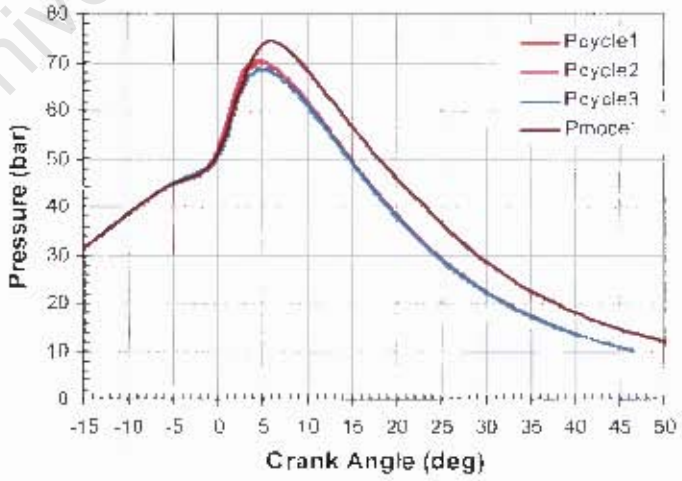

Figure 4-8: Methanol fuelled HCCI pressure profile at λ = 4; CR 19.55:1; 1 bar; 390 K; 0% EGR and 1000 rpm with improved correlations

The following figures 4-9 to 4-11 show the comparison of the model and experimental total heat release.

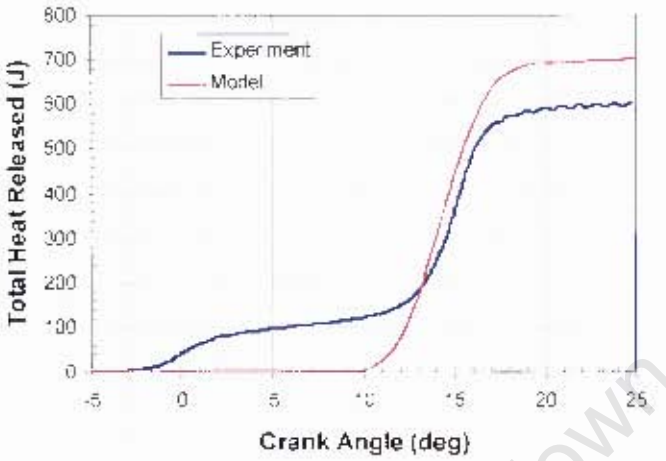

Figure 4-9: Comparative total heat release for n-heptane HCCI combustion at λ = 2; CR 7.95:1; 1 bar; 340 K; 0% EGR and 1000 rpm

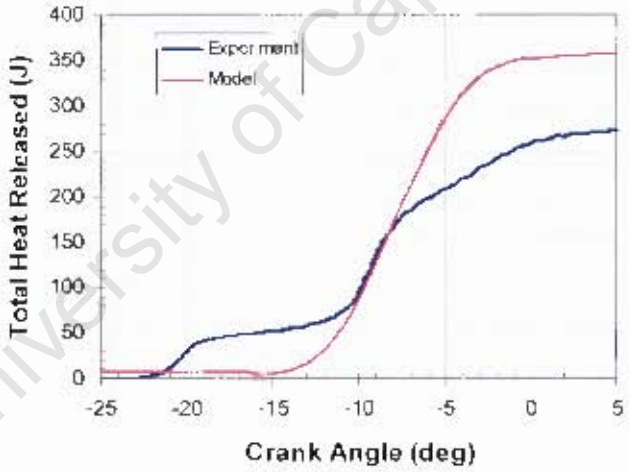

Figure 4-10: Comparative total heat release for n-heptane HCCI combustion at λ = 4; CR 14.0:1; 1 bar; 340 K; 0% EGR and 1000 rpm

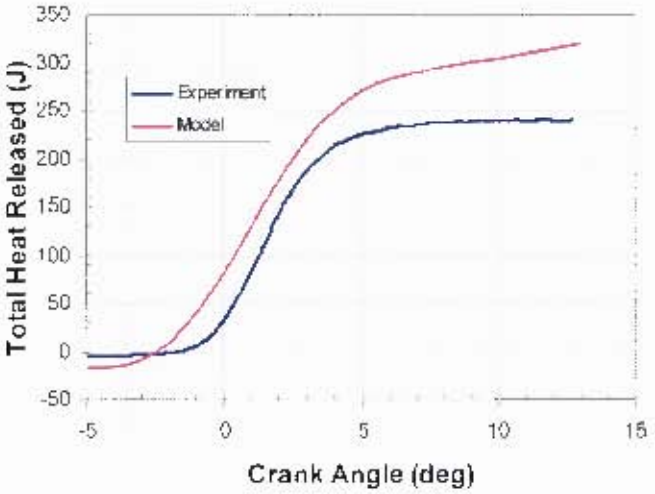

Figure 4-11: Comparative total heat release for methanol HCCI combustion at λ = 4; CR 19.55:1; 1 bar; 390 K; 0% EGR and 1000 rpm

The graphs above show clearly the differences between the model and experimental heat release. The first observed difference was the omitted low temperature heat release in the model predictions of n-heptane. The total heat released in the model predictions were higher that the experimental results. This can be attributed to the absence of inhomogeneity in the model, which exists in real engines and the assumption of complete evaporation of the in-cylinder mixture. It was observed that the error in the cumulative heat release of n-heptane predictions became more pronounced as the mixture leaned out. This was associated with assumption of complete combustion (i.e. 100% combustion efficiency), which is not necessarily true in real engines. Nevertheless, the predictions of the heat release rates correlated well with the experimental results.

The improvements in the Woschni and burn duration correlations improved the model predictions of the SOC and HRR (heat release rate) quite significantly. However, the model still over predicts the peak cylinder pressure, but this was not a big concern at this stage of fuel design. This was not unexpected because it is well known that zero-dimensional models over predicts peak pressure due to the strict simplifying assumption of homogeneity (Zhao et al., 2003). The model was now ready to be used as a tool for analysing HCCI combustion.

4.2 Sensitivity Study

In this section a sensitivity study on the ignition model was conducted due to uncertainties in the ignition delay parameters that characterise a fuel. The study focused on the effect of varying the nine parameters of the ignition delay model and their implications on the prediction of combustion phasing. The ignition delay parameters of n-heptane were chosen as the basis of analysis and the results are presented below.

In figure 4-12 the constant of proportionality, A_i was varied by 10% from its original value for each stage. The result of this study shows that an increase (10%) in the value of A_i would promote a late ignition of the mixture in the cylinder that might result in misfire, due to the increased ignition delay. On the other hand, a decrease in the constant of proportionality would result in very early ignition of the in-cylinder mixture due to the significant reduction in ignition delay.

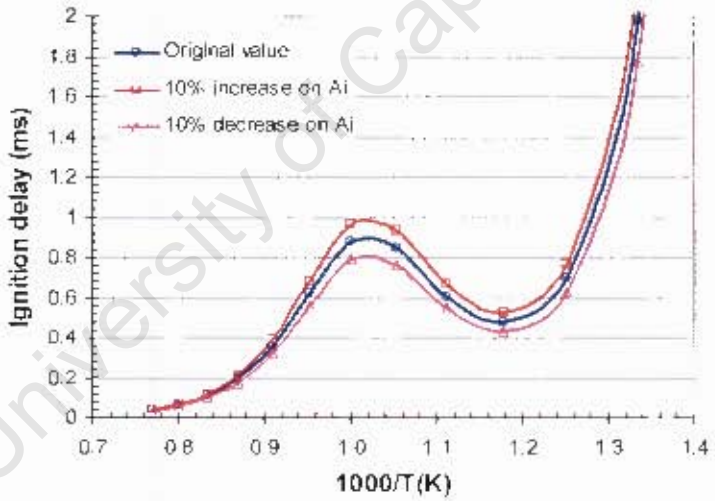

Figure 4-12: Effect of 10% variation of the proportionality constants, A_i, at 40 bar and $\lambda = 1$

Figure 4-13 shows the effects of 10% variation of the pressure coefficients, n_i. The results showed that the effect of the variation was insignificant in the low temperature regime and more pronounced in the intermediate and high temperature regime. Although these results were less pronounced compared to the effect of the constant of proportionality, an increase in the pressure coefficients would retard autoignition, whereas a decrease would advance autoignition.

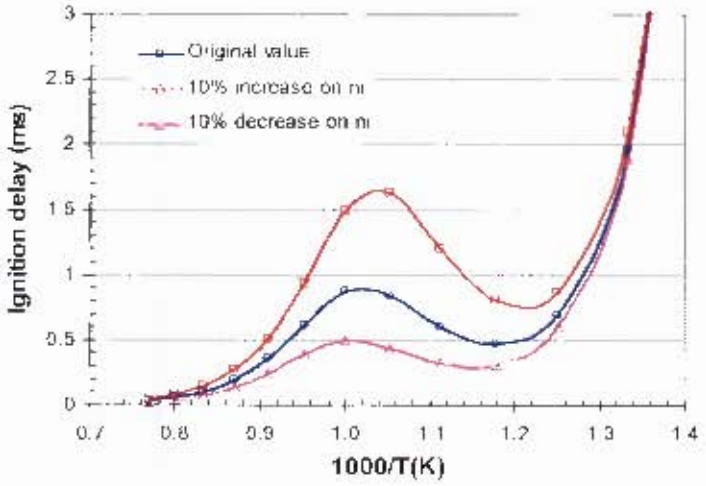

Figure 4-13: Effect of 10% variation of the pressure coefficients, n_i, at 40 bar and λ = 1

Figure 4-14 shows similar results to the variation of the proportionality constants however, the effect of 10% variation of the temperature coefficients was more pronounced. An increase would dramatically retard combustion phasing and could result in misfire, whilst a decrease could significantly advance start of combustion and could result in undesirable early ignition during compression stroke.

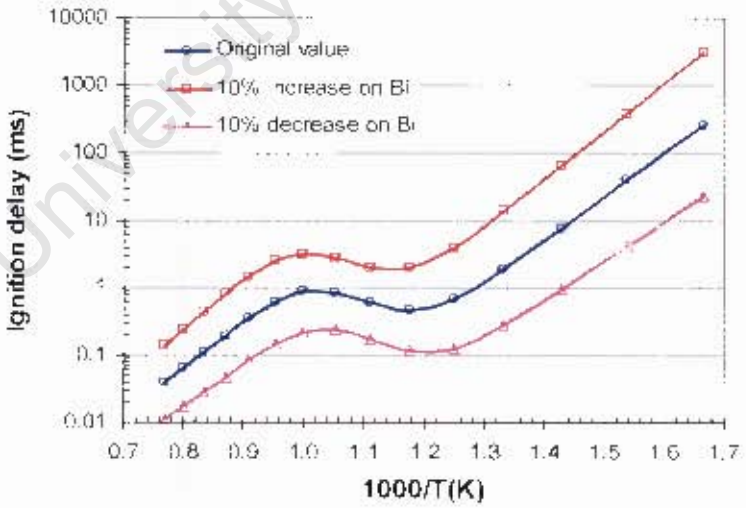

Figure 4-14: Effect of 10% variation of the temperature coefficient, B_i, at 40 bar and λ = 1

Figure 4-15 shows the effect of 10% variation of the pressure coefficient on the modelled pressure profile. It was observed from the graph that the start of main heat release was

advanced when the value of n was decreased and retarded when n_i was increased by 10%. For the same condition misfire was encountered when the temperature coefficient was increased by 10%.

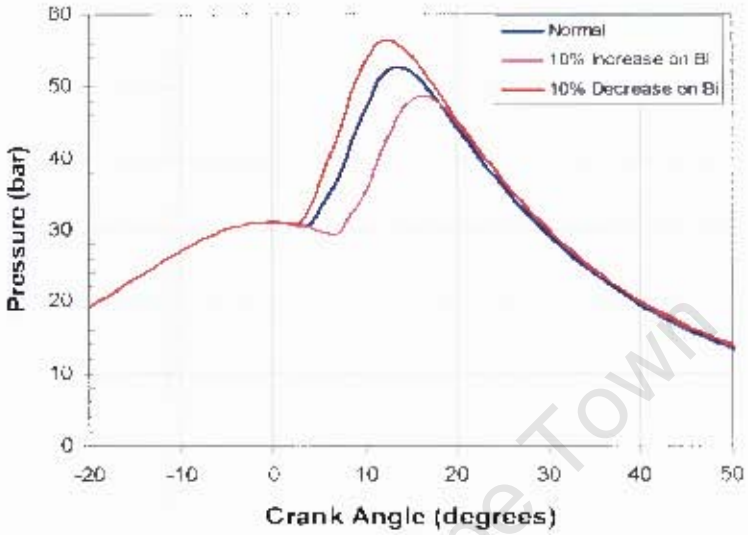

Figure 4-15: Effect of 10% variation of the pressure coefficient n_i at 1000 rpm, 1 bar, 300 K, 13:1, 0% EGR and equivalence ratio of 0.3

It is very important to accurately predict the ignition delay parameters that characterise each fuel component. Any incorrect prediction of the parameters particularly the temperature coefficient would result in misfire or very early ignition during compression stroke. Despite the outcomes of this study, it was assumed that the ignition delay parameters of the fuel components used in this project were accurately predicted.

4.3 *Effect of inlet parameters*

Different inlet parameters were varied to check the sensitivity of the model to the change in inlet conditions. The effect of each parameter was studied and the results obtained were verified against literature. The parameters that were change and their effects are discussed in details below. For each test, different conditions were selected for the best demonstration of the goal being achieved.

4.3.1 Inlet Temperature

The intake manifold temperature was varied from 300 K to 450 K, with all the other inlet manifold conditions kept constant as shown in Table 4-1. The model was used with n-heptane as fuel to predict the start of combustion (SOC) as well as to investigate the sensitivity of the model to changes in inlet temperature. Figure 4-16 shows the effect of inlet temperature on HCCI combustion fuelled with n-heptane.

Parameter	Value and units
Engine Speed	2500 rpm
Intake Manifold Pressure	1 bar
Intake Manifold Temperature	Varied
Air/Fuel ratio (lambda λ)	4
Compression ratio	15:1
Exhaust gas recirculation (EGR)	0 %
Fuel	n-Heptane

Table 4-1: Engine conditions for inlet temperature sensitivity test

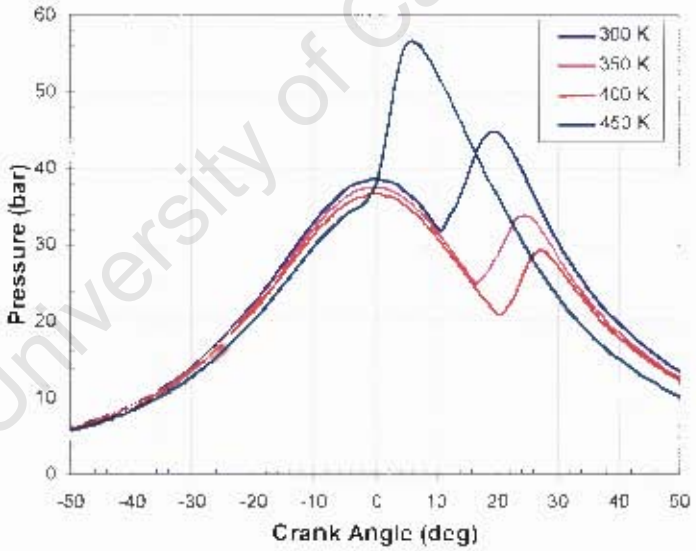

Figure 4-16: Effect of inlet temperature on HCCI combustion at 1 bar inlet pressure, 15:1 compression ratio, 0% EGR, 0.25 equivalence ratio and 2500 rpm engine speed

As the inlet temperature was increased the compression pressures were reduced. This effect was clearly observed in pressure traces in figure 4-16. This was attributed to the different inlet temperatures and the increased amount of heat loss in the cylinder due to the increased inlet temperatures. It was also observed from the graph that the SOC was retarded as the

inlet temperature increased until a certain point and then advanced again. One would expect an increase in inlet temperature to advance the combustion phasing, which is not what was observed in the results. There is a logical explanation for the cause of delay in the predicted SOC. N-heptane is one of the fuels that exhibit strong negative temperature coefficient (NTC) behaviour as shown in figure 4-17.

Increasing the intake manifold temperature at constant inlet pressure resulted in the cylinder temperatures reaching the intermediate temperature regime. As explained in chapter 2 that ignition delay tends to be longer as the temperature increases in the NTC regime. This was observed when the inlet temperature was increased from 300 K to 400 K and beyond 400 K, ignition delay decreased with increasing inlet temperature. Figure 4-17 shows the movement of the start of combustion along the ignition delay curve of n-heptane as the inlet temperature was increased.

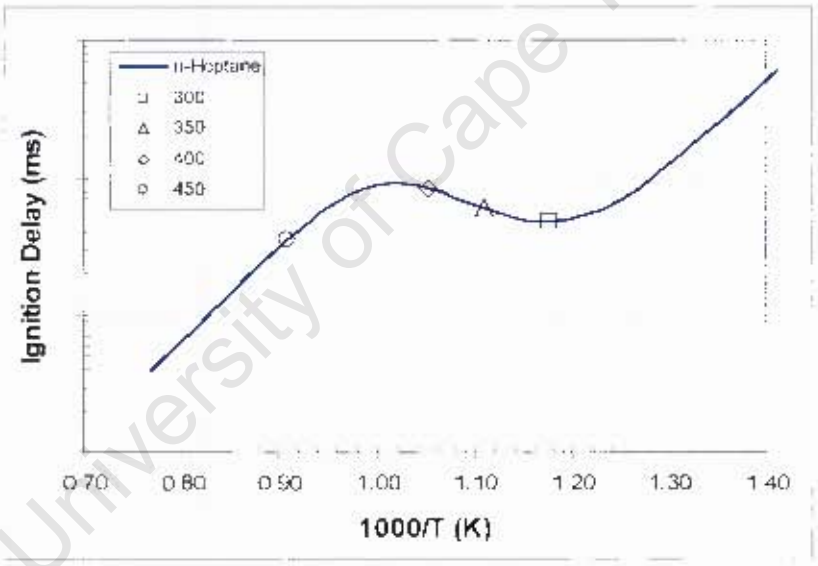

Figure 4-17: Ignition delay (ms) for n-Heptane at 40 bar, λ =1 and 0% EGR

4.3.2 Compression Ratio

The model proved to be sensitive to compression ratio changes as expected. The results for this are shown in Figures 4-1 to 4-5 and 4-18. As expected, the burn duration became shorter and the combustion phasing was advanced as the compression ratio was increased. This can be attributed to the fact that an increase in compression ratio results in an increase

in temperature and pressure under compression and expansion. The compression ratio effect on the pressure profiles is clearly shown in figure 4-18 below.

In figures 4-1 to 4-5, the compression ratio was used as a means to control combustion phasing. A high compression ratio was used for very lean mixture and reduced as the mixture became richer to limit the heat release rate (HRR).

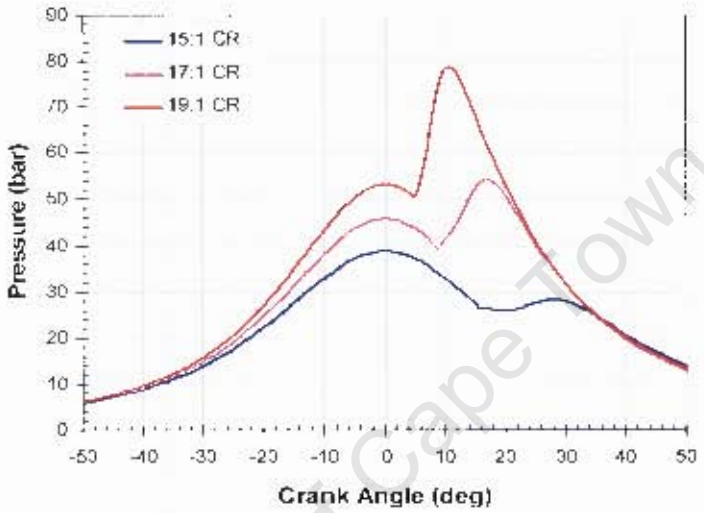

Figure 4-18: Effect of compression ratio on HCCI combustion at 1 bar inlet pressure, 300 K inlet temperature, 0% EGR, 0.25 equivalence ratio and 3000 rpm engine speed

4.3.3 Fuel-Air Equivalence Ratio

The fuel-air equivalence ratio (Φ) was varied from 0.2 to 0.5 by varying the fuel quantity at the same inlet conditions (inlet pressure 1 bar, inlet temperature 340 K, compression ratio 11:1) and engine speed (1000 rpm) with 0% EGR. The indicated mean effective pressure (IMEP) was observed to increase with equivalence ratio and the indicated thermal efficiency decreased. This resulted from the increased fuel concentration in the cylinder. The results are shown in figure 4-19 and are in good agreement with the literature (Noel et al., 2004).

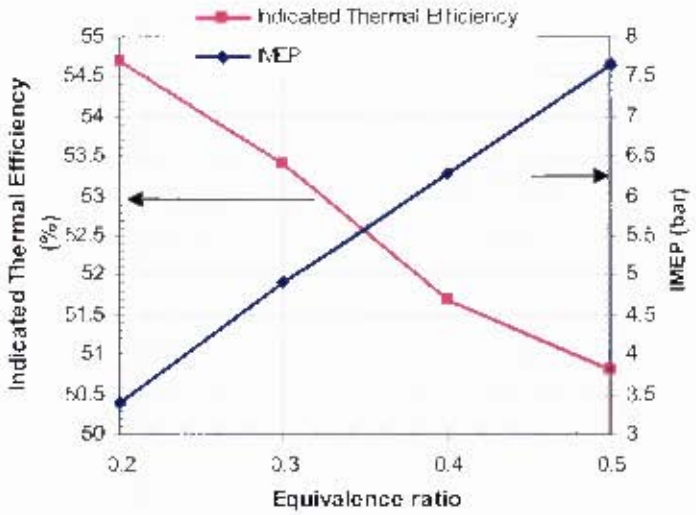

Figure 4-19: Effect of equivalence ratio on IMEP and indicated thermal efficiency at 1 bar inlet pressure, 340 K inlet temperature, 11:1 compression ratio, 0% EGR and 1000 rpm engine speed

In figures 4-20 and 4-21 below, the combustion duration was observed to decrease as the equivalence ratio increased. Furthermore, an increase in equivalence ratio advanced the SOC and the HRR was increased leading to high cylinder pressures. The total amount of heat release also increased with equivalence ratio. All this resulted from the increased amount of fuel inducted in the cylinder. These results show the reason why lean burn is preferred for HCCI combustion.

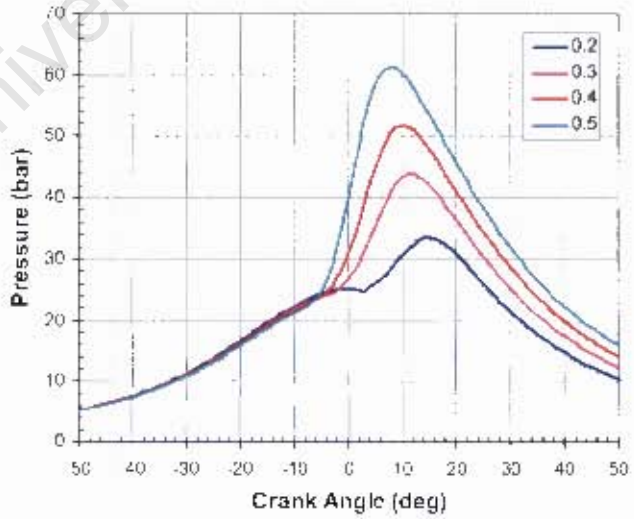

Figure 4-20: Effect of equivalence ratio (Φ) on HCCI combustion at 1 bar inlet pressure, 340 K inlet temperature, 11:1 compression ratio, 0% EGR and 1000 rpm engine speed

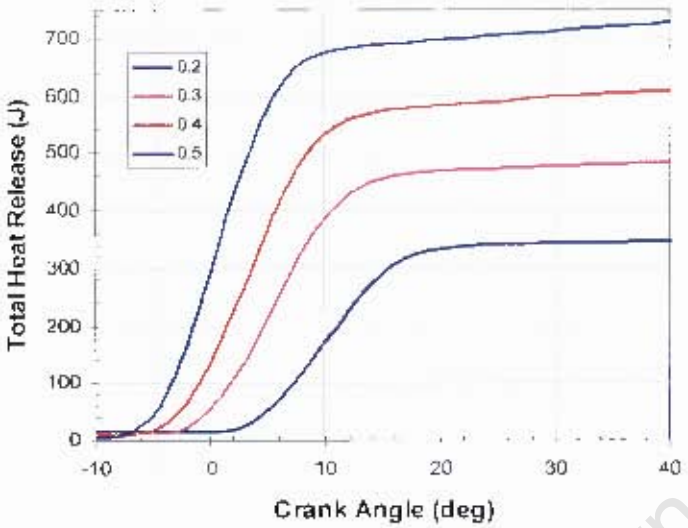

Figure 4-21: Effect of equivalence ratio on total heat release at 1 bar inlet pressure, 340 K inlet temperature, 11:1 compression ratio, 0% EGR and 1000 rpm engine speed

4.3.4 Exhaust Gas Recirculation

The effect of EGR on HCCI combustion has been verified by increasing EGR rates from 0% to 50% for the same conditions given in section 4.3.3, except that the compression ratio was change to 15:1 and an inlet equivalence ratio of 0.3 was used. It was observed that charge dilution decreased IMEP and increased the indicated thermal efficiency (see Figure 4-22). This was attributed to the decreased amount of fuel in the cylinder as EGR rates increased. Figure 4-23 shows the effect of EGR on the in-cylinder pressure development. The SOC was delayed and the peak cylinder pressures were reduced by the charge dilution. These results on the effect of cooled EGR on HCCI combustion are in good agreement with literature (Olsson et al., 2003).

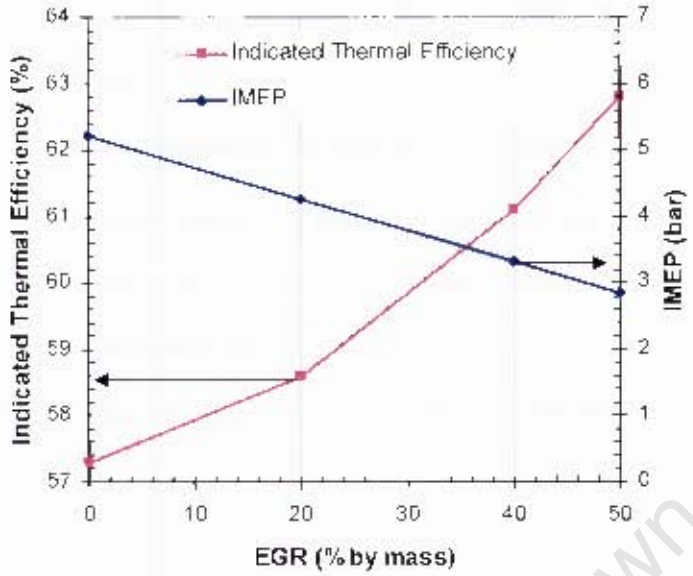

Figure 4-22: Effect of EGR rate on IMEP and indicated thermal efficiency at 1 bar inlet pressure, 340 K inlet temperature, 15:1 compression ratio, 0.3 equivalence ratio and 1000 rpm engine speed

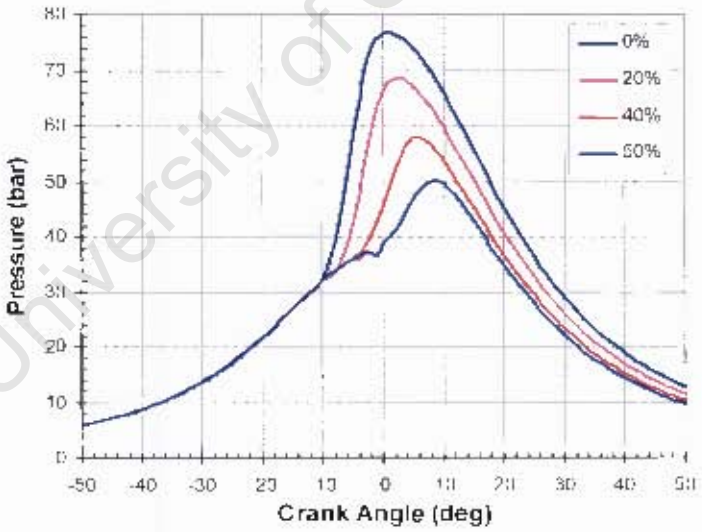

Figure 4-23: Effect of EGR on HCCI combustion at 1 bar inlet pressure, 340 K inlet temperature, 15:1 compression ratio, 0.3 equivalence ratio and 1000 rpm engine speed

4.3.5 Inlet Pressure

With the same conditions (inlet temperature 320 K, compression ratio 11:1, 0.25 equivalence ratio and 1000 rpm engine speed with 0% EGR) the inlet pressure increased to 2 bar in steps of 0.5 bar via a supercharger to investigate its effect. Figure 4-24 shows that the combustion phasing was advanced and HRR was increased resulting to high peak pressures and IMEP. Table 4-2 shows the effect of forced induction on IMEP, indicated thermal efficiency and mechanical efficiency. Figure 4-25 shows the comparison of the pressure profiles as the boost pressure was increased.

Boost Pressure (bar)	IMEP (bar)	Indicated Thermal Efficiency (%)	Mechanical Efficiency (%)
0	4.37	53.5	68.1
0.5	6.98	57.5	41.8
1	9.82	60.6	30.8

Table 4-2: Effect of boost pressure on IMEP and indicated thermal efficiency at 320 K inlet temperature, 11:1 CR, 0.25 equivalence ratio and 1000 rpm with 0% EGR

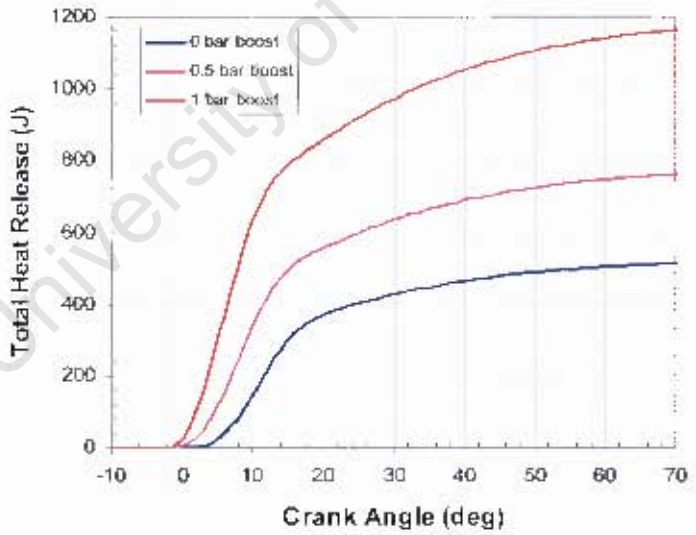

Figure 4-24: Effect of boost pressure on total heat release at 320 K inlet temperature, 11:1 CR, 0.25 equivalence ratio and 1000 rpm with 0% EGR

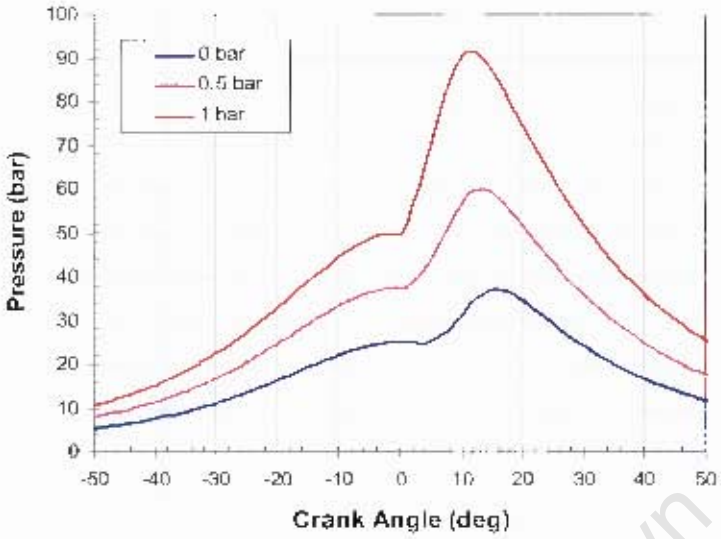

Figure 4-25: Effect of boost pressure on HCCI combustion at 320 K inlet temperature, 11:1 compression ratio, 0.25 equivalence ratio and 1000 rpm engine speed with 0% EGR

The work done per cycle increased as the inlet pressure was increased, thus resulting in the observed increase in IMEP and indicated thermal efficiency. However, the cost of boosting was observed as a drop in mechanical efficiency. The reduction in mechanical efficiency was attributed to the increased fMEP, which resulted from the required compressor work and intercooler heat transfer during for forced induction (see equation 3-9). The combustion duration was observed to decrease as the boost pressure increased, due to the increased amounts of fuel-air mixture in the cylinder (Noel et al., 2004).

4.4 Known Fuels Study

The procedure followed in obtaining the results discussed in this section is given in section 3.4.2 of chapter 3.

4.4.1 Effect of Fuel Properties and Octane Rating

Although methanol could not be ignited at 390 K inlet temperature, compression ratio 15:1 and relative air-fuel ratio of 2, when ignition occurred yielded the best performance results compared to other fuels tested. These results were in agreement with the findings of

Aroonsrisopon et al. (2002), Ogawa et al. (2003) and Oakley et al. (2001) who reported that methanol exhibited good HCCI combustion characteristics and widened HCCI engine operating range.

Toluene was also used as fuel in the model, but no combustion occurred for the test conditions given in table 3-4. This was attributed to the high activation energy required to abstract hydrogen (H) from primary carbon sites and absence of low temperature reactions, which reduce the overall ignition delay. For combustion to occur within 10 crank angle degrees (CAD) of top dead centre (TDC) with toluene as fuel, the compression ratio had to be increased to at least 21.3:1. The comparisons of the fuels that ignited in the conditions given in table 3-4 are shown below in tables 4-3 to 4-5 and figures 4-26 to 4-28.

Fuel	Indicated Mean Effective Pressure (bar)	Mechanical Efficiency (%)	Indicated Thermal Efficiency (%)
N-Heptane	3.24	3.79	48.32
Iso-Octane	3.57	12.97	53.60
1-Hexene	4.11	24.48	60.0
Methanol	4.80	37.68	66.78

Table 4-3: Model engine performance results for the different test fuels at λ = 4, 390 K and 18:1 compression ratio

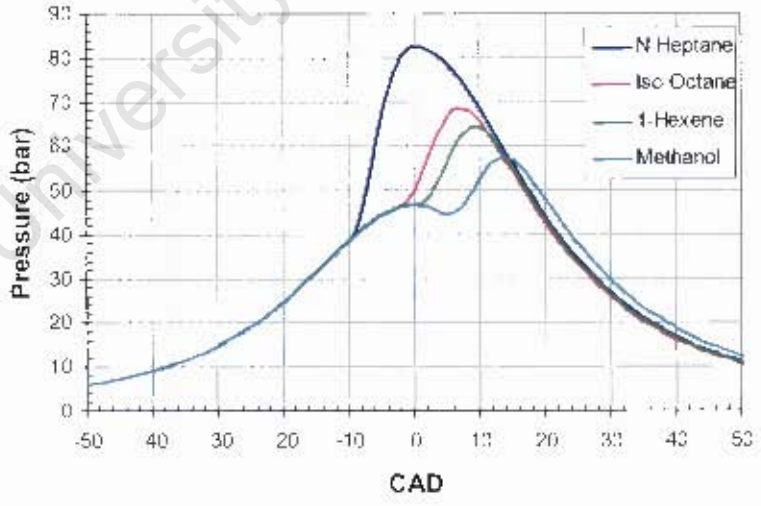

Figure 4-26: Comparison of model cylinder pressures fuels at λ = 4, 390 K and CR 18:1

Fuel	Indicated Mean Effective Pressure (bar)	Mechanical Efficiency (%)	Indicated Thermal Efficiency (%)
N-Heptane	6.91	54.3	52.2
Iso-Octane	6.92	62.5	52.3
1-Hexene	7.23	61.9	53.5
Methanol	No combustion		

Table 4-4: Model comparative performance results at λ = 2, 390 K and 15:1 compression ratio

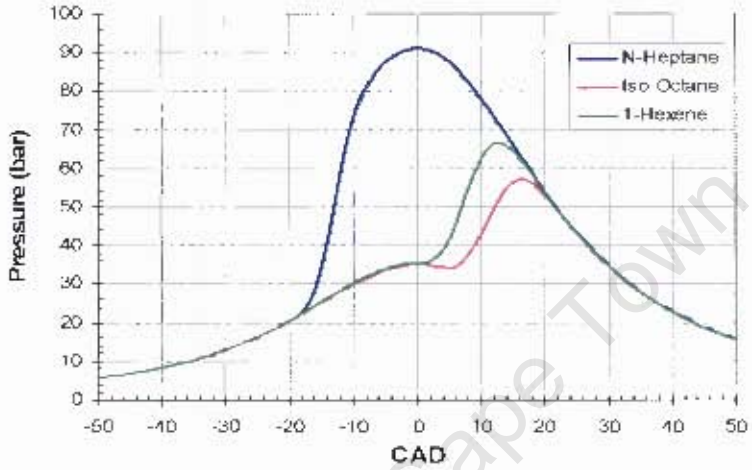

Figure 4-27: Comparative pressure profiles at λ = 2, 390 K and 15:1 compression ratio

Fuel	Indicated Mean Effective Pressure (bar)	Mechanical Efficiency (%)	Indicated Thermal Efficiency (%)
N-Heptane	6.50	49.9	55.1
Iso-Octane	6.90	55.8	54.5
1-Hexene	7.05	56.3	54.4
Methanol	7.24	62.2	55.1

Table 4-5: Model performance results at λ = 2, 410 K and 15:1

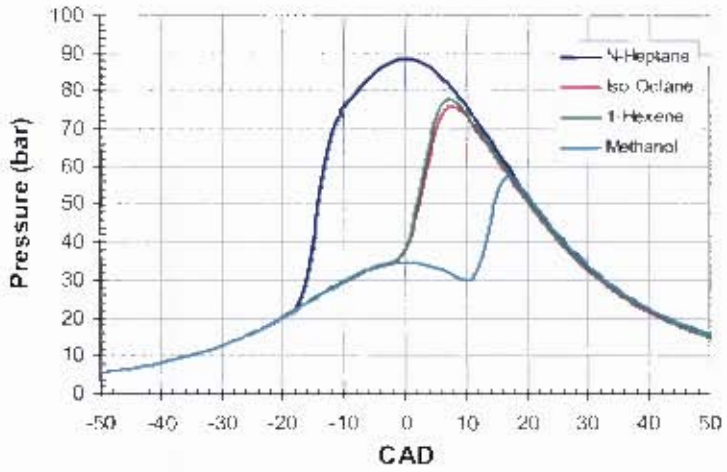

Figure 4-28: Comparative pressure traces at λ = 2, 410 K and 15:1

It was observed in figures 4-26 to 4-28 and tables 4-3 to 4-5 that HCCI combustion was affected by fuel properties and autoignition properties. In general, the IMEP and efficiencies were observed to increase in the order: n-heptane < iso-octane < 1-hexene < methanol. The octane rating of the fuel components increased in the order: n-heptane < 1-hexene < iso-octane < methanol. There was no consistent correlation found between the ON of the different classes of fuels and the engine performance. However, in the case of primary reference fuels (PRF) ignition delay increases with decreasing RON (research octane number).

For a given set of operating conditions, a high octane fuel can realise higher IMEP and efficiencies than a low octane PRF provided that it autoignites. This finding was in agreement with the conclusion of Yao et al. (2004). Furthermore, Aceves et al. (2003) concluded that fuels with relatively low octane number cannot operate at high compression ratio unless the intake mixture is cooled below ambient temperature. This was observed for n-heptane in figure 4-26 to 4-28, early SOC during compression stroke resulting in high peak pressures and low mechanical efficiency.

The sensitivity of the fuels increased in the order: n-heptane = iso-octane < 1-hexene < methanol, as calculated from equation 3-14. This order correlates well with the order in which the IMEP and efficiencies increase. Therefore, a more sensitive fuel results in high efficiencies. This effect of fuel sensitivity on HCCI combustion can be associated to the

thermodynamic and autoignition properties of the fuel. For example, methanol has the lowest heating value and the highest specific density compared to other fuel components. Therefore, methanol can yield higher efficiencies compared to other fuels and this was observed in this study.

The mechanical efficiencies in table 4-4 seem to contradict with the order presented above. This can be explained by comparing the pressure traces of iso-octane and 1-hexene. In figure 4-26 1-hexene ignited late compared iso-octane, whereas in figure 4-27 the opposite was observed. Basically, the ignition delay of 1-hexene is shorter that the ignition delay of iso-octane in the low-intermediate temperature regime and longer in the high temperature regime (see figure C-2 in Appendix C). This could attribute to the observed differences in the start of combustion of iso-octane and 1-hexene as the inlet conditions were varied. Any fuel that ignites early compared to the other results in higher peak pressures, as observed in the graphs. Therefore, the discrepancies in the efficiencies can be attributed to the increased fMEP due to the increased peak pressure (see equation 3-9).

4.4.2 N-Heptane Load Map

The surface below, figure 4-29, shows the effect of EGR and fuel-air equivalence ratio on IMEP and was very useful in determining the combinations of EGR and equivalence ratio at a given speed for different loads. Similar surfaces were obtained for 3000 rpm and 5000 rpm.

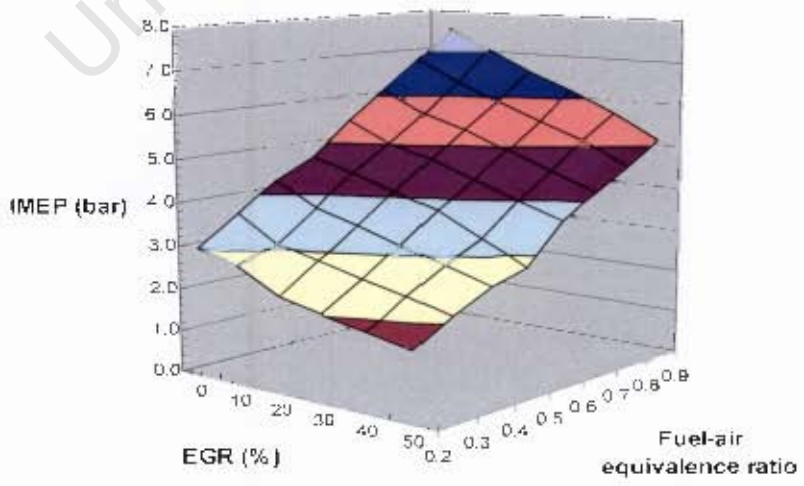

Figure 4-29: Effect of EGR and equivalence ratio on IMEP at 1000 rpm

Table 4-6 shows the possible EGR and equivalence ratio combinations as well as corresponding efficiencies at the given speed range (1000 to 5000 rpm) and 25% load. It was clear from the table that efficiency remains relative constant at given speed, for any suitable combination of equivalence ratio and EGR. It was observed in table 4-6 that the mechanical efficiency dropped with increasing engine speed. This was attributed to friction since the friction mean effective pressure (fMEP) increased with engine speed. Moreover, reduction in mechanical efficiency represented the penalty of boost pressure, which increased with engine speed (see equation 3-16).

BMEP = 2.05 bar (25% load) and N = 1000 rpm			**BMEP = 2.17 bar (25% load) and N = 3000 rpm**			**BMEP = 2.06 bar (25% load) and N = 5000 rpm**		
ϕ	**EGR (%)**	η_{mech} **(%)**	ϕ	**EGR (%)**	η_{mech} **(%)**	ϕ	**EGR (%)**	η_{mech} **(%)**
0.50	-	-	0.44	0.00	28.4	0.40	0.0	19.5
0.51	0.0	44.0	0.49	10.0	28.7	0.45	10.0	19.2
0.56	10.0	43.9	0.50	12.4	28.8	0.50	19.0	19.6
0.60	18.0	44.1	0.57	20.0	30.5	0.51	20.0	19.6
0.61	20.0	44.1	0.60	22.3	31.3	0.58	30.0	19.7
0.67	30.0	44.0	0.67	30.0	31.5	0.60	31.8	19.8
0.70	33.7	44.1	0.70	32.6	31.5	0.69	40.0	19.9
0.74	40.0	43.9	0.76	40.0	32.2	0.70	41.5	20.0
0.80	46.5	44.0	0.80	45.1	33.3	0.80	49.8	20.8
0.84	50.0	44.0	0.89	50.0	33.2	0.80	50.0	20.8

Table 4-6: Possible combinations of EGR and equivalence ratio (Φ) and the resulting corresponding mechanical efficiencies (η_{mech}) at each speed and 25 % load

These results were obtained for each load up to 100% load and for each speed the combination that gave the best efficiency was selected. The results of the best efficiencies at each load are shown in table 4-7 below.

High loads could not be achieved at low speeds because combustion occurred very early with short combustion duration. This can be attributed to the simplifying assumptions of complete evaporation of fuel and homogeneity. The maximum load that could be attained at 1000 rpm was 57% (i.e. 4.67 bar IMEP) and the maximum load obtained at 3000 rpm was 77% (i.e. 6.68 bar IMEP). It was possible operate at 100% load at 5000 rpm with 0.25 bar boost pressure as seen in table 4-7. This was possible because of the late start of ignition and slightly longer burn duration at high speeds.

The heat release rates were observed to be very high at high load. The rates of pressure rise per crank angle degree ($dP/d\theta$) were more than 10 bar/CAD, which was defined as the knock

limit (see table 4-7). Therefore, high loads were achieved with the engine severely knocking, because the pressure rise rates were almost double the knock limit. The ideal load map is shown in figure 4-30 with n-heptane fuel and without considering engine knock. Engine knock results from the high pressure rise rates due to short combustion duration. If taking engine knock into consideration, the maximum attainable load was reduced to at most 45% (i.e. 3.9 bar bMEP). Therefore, to overcome this problem, some form of non-chemical duration elongation is required.

N (rpm)	Load (%)	ϕ	EGR (%)	boost (bar)	η_{imech} (%)	dp/dθ (bar/CAD)
1000	25	0.6	17.9	0	44.1	5.5
	50	0.9	12.9	0	61.2	18.3
	57	0.9	0.7	0	64.3	23.3
	75	-	-	-	-	-
3000	25	0.8	45.1	0.55	33.3	8.1
	50	0.8	18.0	0.18	48.9	12.2
	75	0.9	2.2	0	59.0	21.6
	100	-	-	-	-	-
5000	25	0.8	50.0	1.14	20.8	7.4
	50	0.8	32.3	0.96	35.8	10.7
	75	0.9	20.4	0.74	49.6	16.7
	100	0.9	4.2	0.25	61.3	20.3

Table 4-7: Most efficient operating conditions at each load point and speed

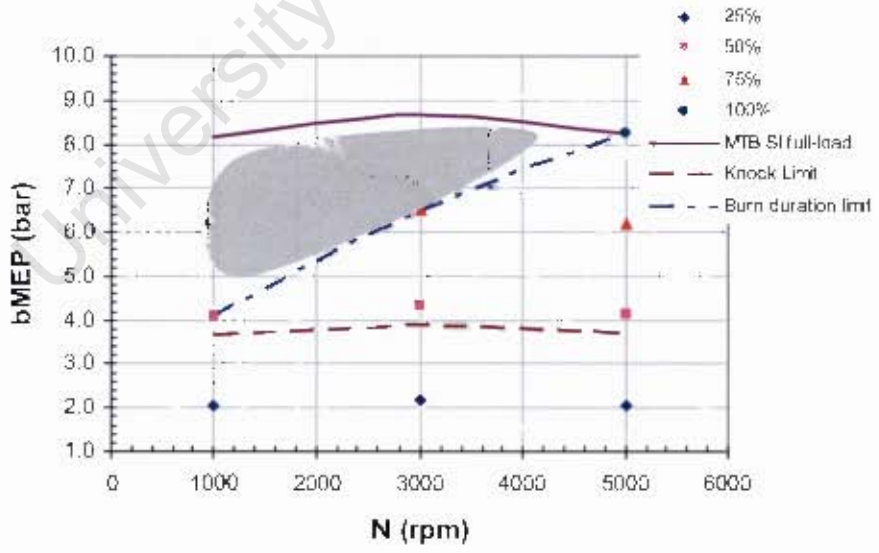

Figure 4-30: Ideal HCCI load map for n-heptane without considering engine knock

The model could not be operated in the shaded region between the MTB of SI full-load line and the burn duration limit line. Early combustion phasing during compression stroke and short combustion duration limited operation in shaded region. This resulted in combustion completing before TDC, thus reducing the output of the engine model. It would be possible to operate the engine model in the shaded region, if the combustion phasing is retarded and the combustion duration is lengthened without compromising the IMEP. The possible technique that could retard timing and prolong burn duration was EGR, but its penalty was a reduction in IMEP. However, a combination of other approaches discussed in chapter 2 could solve the problem.

4.5 Fuel design

The barriers for operating in the full load range were established to be the following:

- Knocking at high loads
- Misfire at low loads
- Fast combustion at low speeds
- Slow combustion or none at high speeds

These were the barriers that had to be overcome to ensure stable HCCI operation in the entire load-speed range. These barriers lead to the following requirements for the fuel:

- Fuel must readily autoignite at all speeds
- Mitigate the high rates of heat release at high loads

The methodology followed in the design of the ignition delay characteristics of the designer fuel is given in section 3.4.3.

4.5.1 Compression Ratio Study

The first step prior to design of the fuel was to investigate the effect of compression ratio on the final fuel characteristics. This was done by obtaining pressure and temperature data at the conditions discussed in section 3.4.3 for three compression ratios; 10:1, 17:1 and 24:1. Figure 4-31 below shows the comparative results of this compression ratio study.

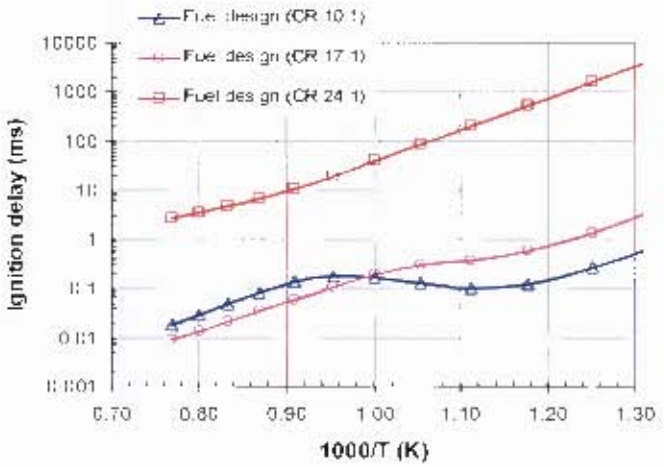

Figure 4-31: Effect of compression ratio on ignition delay characteristics at 40 bar for the fuel design

It was clear from the graph that compression ratio had a huge impact on the final fuel characteristic. The design for high compression ratios would result in the difficulties to obtain autoignition at low compression ratios. Likewise, design for low compression ratios would result in knock at high compression ratio operations. The remaining option was to find an intermediate compression ratio that would enable HCCI operation at low and high compression ratios. This intermediate compression ratio was obtained to 15:1 using the trial and error method.

4.5.2 The Designer Fuel

Based on the outcomes of the compression ratio study, it was decided to control combustion phasing at low compression ratios and high compression ratios by changing other inlet parameters such as temperature, EGR and pressure. The compression ratio of 15:1 and inlet temperature of 300 K were selected for the design of the final characteristics of the designer fuel. The following figures 4-32 and 4-33 show the comparison of the ignition delay characteristics of the design fuel with toluene and n-heptane fuel at 12 bar and 40 bar.

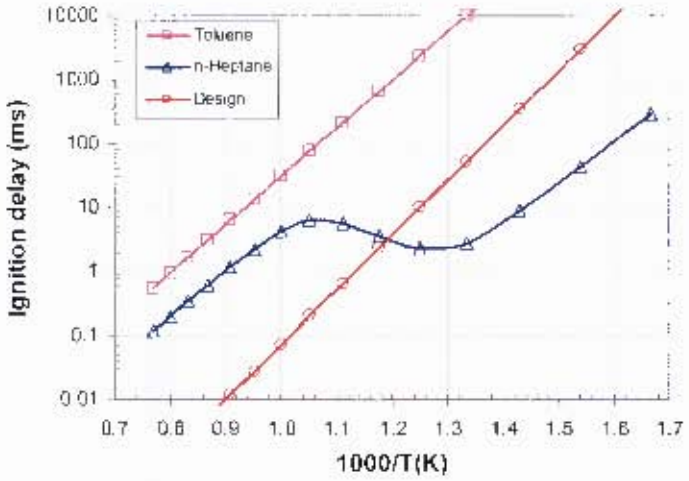

Figure 4-32: Comparison of the design fuel with toluene and n-heptane at 12 bar

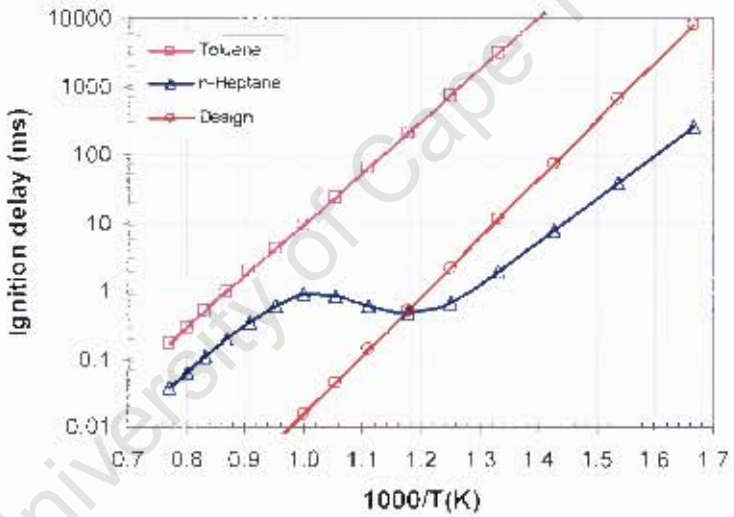

Figure 4-33: Comparison of the design fuel with toluene and n-heptane at 40 bar

It was clear from the graphs that a fuel with single-stage ignition was required in order to extend the load and speed range of an HCCI combustion engine. The fuel offered dramatically reduced ignition delay compared to toluene throughout the temperature and pressure range. Compared to n-heptane, it provided longer ignition delays for temperatures approximately less than 800 K and significantly shorter ignition delays for temperatures above 800 K. This could be attributed to the requirement for the fuel to autoignite throughout the speed range without forced induction.

These results were not unexpected, because Zhao et al. (2003) stated that fuels with single-stage ignition are less sensitive to load and speed changes, and that can ease the requirements on the control systems over a wide range of engine parameters.

The thermodynamic and physical properties of the designer fuel were not evaluated, but only the autoignition characteristics were known. For the purpose of testing the fuel, the thermodynamic properties were assumed to be similar to those of conventional hydrocarbon fuels.

5 Conclusion

The conclusions that were reached based on the foregoing information can be summarized as follows:

- A simple mathematical model that could be used as a tool to simulate HCCI combustion was developed and validated against experimental data. Although some autoignition features of hydrocarbon fuels were approximated due to the simplicity of the model, it proved possible to predict the start of main heat release within reasonable accuracy. Moreover, the model produced results that were in good agreement with literature and experiment.

- There was insufficient data in the literature to develop and calibrate a suitable combustion duration correlation. The combustion duration was therefore inferred from the experimental Ricardo E6 data.

- Inaccurate calibration of the ignition delay characteristic parameter would result in a significant retard, which would lead to misfire or advance of the predicted combustion phasing, which would lead to engine knock.

- The compression ratio was identified as one of the most important parameters when designing a fuel for HCCI combustion. For example, if the fuel was designed for low compression ratios and used at high compression ratios engine knock would occur and surely misfire would occur for the opposite condition.

- With a suitable compression ratio, it was possible to conceive a designer fuel with single-stage ignition characteristics, which could be operated throughout the load and speed range. Only the autoignition characteristics of the fuel were identified at this stage; the required thermodynamic and other properties were not evaluated. Such a fuel would allow HCCI combustion throughout the speed range (1000 – 5000 rpm) and load range ($0.2 \leq \Phi \leq 1$) without forced induction. However, high peak pressures and heat release rates would be inevitable at high loads ($\Phi > 0.5$).

6 Recommendations

On the basis of the abovementioned conclusions, the following recommendations are made:

- Currently the combustion model does not include the heat release during low temperature oxidation, even though the ignition delay model does include the delay associated with cool flames. It is recommended to conduct an investigation on how much heat is released during cool flames and to confirm the association of the start of cool flames with the low temperature ignition delay, τ_1. The findings need to be implemented in the model to improve predictions of combustion phasing of fuels with two-stage ignition.

- Due to the lack of experimental data in the literature to develop a more accurate combustion duration correlation, it is recommended to conduct experiments using different engines and 3-D modelling with different fuels and operating conditions to establish this data and then refine the combustion duration correlation.

- Even small variations (10%) in the calibration of the ignition delay parameters, more especially the temperature coefficient B_i, would promote very early or late autoignition of the in-cylinder mixture. Related to these results, it is strongly recommended to verify the parameters characterising the ignition delay of the designer fuel after the above mentioned recommendations are implemented. This means that more experiments and models are required to verify these characteristic parameters.

- Since only the autoignition characteristics of the fuel were designed, it is recommended to try to match these characteristics with different fuel blends of known fuel components to ascertain its possible thermodynamic and physical properties. An experimental study need to be conducted to investigate the predictions of this modelling study.

7 References

Aceves, S.M., Flowers, D., Martinez-Frias, J., Espinosa-Loza, F., Pitz, W.J. and Dibble, R. (2003) *Fuel and Additive Characterization for HCCI Combustion,* SAE 2003-01-1814 2-8

Aroonsrisopon, T., Sohm, V., Werner, P., Foster, D.E., Morikawa, T. and Iida, M. (2002) *An Investigation into the Effect of Fuel Composition on HCCI Combustion Characteristics,* SAE 2002-01-2830 4-19

Aroonsrisopon, T., Sohm, V., Werner, P., Foster, D.E., Morikawa, T. and Iida, M. 2002. *An Investigation into the Effect of Fuel Composition on HCCI Combustion Characteristics. SAE 2002-01-2830* *1-1*, 3-7

Babajimopoulos, A., Assanis, D., and Fiveland, S.B. 2002. *An Approach for Modeling the Effects of Gas Exhange Processes on HCCI Combustion and Its Application in Evaluating Variable Valve Timing Control Strategies.* SAE 2002-01-2829 2-16

Chang, J., Güralp, O., Filipi, Z., Assanis, D., Kou, T., Najt, P., and Rask, R. (2004) *New Heat Transfer Correlation for an HCCI Engine Derived from Measurements of Instantaneous Surface Heat Flux,* SAE 2004-01-2996 4-3

Christensen, M. and Johansson, B. 1999. *Homogeneous Charge Compression Ignition With Water Injection.* SAE 1999-01-0182 2-6

Christensen, M., Johansson, B., Amneus, P. and Mauss, F. 1998. *Supercharged Homogeneous Charge Compression Ignition.* SAE 980787 2-6

Cox, R.A. and Cole, J.A. 1985. *Chemical Aspects of the Autoignition of Hydrocarbon-air Mixtures.* Combustion and Flame, 60, pp.109-123 2-11

Curran, H.J., Gaffuri, P., Pitz, W.J. and Westbrook, C.K. 1998. *A Comprehensive Modeling Study of n-Heptane Oxidation.* Combustion and Flame, Vol. 114, pp. 149-177 2-12

Douaud, A.M. and Eyzat, P. 1978. *Four-Octane-Number Method for Predicting the Anti-Knock Behaviour of Fuels and Engines,* SAE 780080 2-13

Edward, C.F., Siebers, D.L. and Hoskin, D.H. 1992. *A Study of the Autoignition Process of a Diesel Spray via High Speed Visualization.* SAE 920108 2-10

Epping, K., Aceves, S., Bechtold, R. and Dec, J. 2002. *The Potential of HCCI Combustion for High Efficiency and Low Emissions, SAE 2002-01-1923* *2-1*, 2-2, 2-5

Erlandsson, O., Einewall, P., Johansson, B., Amneus, P. and Mauss, F. 2002. *Simulation of HCCI-Addressing Compression Ratio and Turbo Charging,* SAE 2002-01-2862 2-16

Fiveland, S.B. and Assanis, D.N. (2000) *A Four-Stroke Homogeneous Charge Compression Ignition Engine Simulation for Combustion and Performance Studies,* SAE 2000-01-0332 4-3

Flowers, D., Aceves, S., Smith, R., Torres, J., Girard, J. and Dibble, R. 2000. *HCCI in a CFR Engine: Experiments and Detailed Kinetic Modeling.* SAE 2000-01-0328 2-9

Forst, S. 2005 *Intercoolers.* http://www.nissanperformancemag.com/april05/nerds/. Internet source produced by Forst, S., Nissan Performance Magazine. 3-10

Furutani, M., Ohta, Y., Kono, M. and Hasegawa, M. 1998. *Ultra-Lean Premixed Compression Ignition Engine Concept and its Characteristics.* Preceedings of the Fourth International Symposium COMODIA 98, pp. 173-177 2-8

Griffiths, J.F., 1995. *Reduced Kinetic Models and Their Application to Practical Combustion Systems.* Prog. Energy Combustion Science, Vol. 21, pp25-107 2-12

Griffiths, J.F., Schreiber, M., Sadat Sakak, A. and Lingens, A. 1994. *A Reduced Thermokinetic Model for the Autoignition of Fuels with Variable Octane Ratings.* Twenty-fifth Symposium (Int.) on Combustion, The Combustion Institute, p. 933-940 2-11

Halstead, M.P., Kirsch, L.J. and Quinn, C.P. 1977. *The Autoignition fo Hydrocarbon Fuels at High Temperature and Pressure – Fitting of a Mathematical Model.* Combustion and Flame 30, p. 45-60 2-11

Haraldsson, G., Tunestål, P., Johansson, B. and Hyvönen, J. 2002. *HCCI Combustion Phasing in a Multi Cylinder Engine Using Variable Compression Ratio.* SAE 2002-01-2858 2-5

Heywood, J.B. 1988. *Internal Combustion Engine Fundamentals* (International Edn.). Singapore, McGraw-Hill Book Company passim

Hiraya et al. 2001. *A Study of Gasoline Fueled Compression Ignition Engine – A Trail of Operation Region Expansion,* Preceedings of the JSAE Convention (in Japanese), No. 98-01, p. 9-11 2-6

Ishibashi, Y. and Asai, M. 1996. *Improving the Exhaust Emissions of Two-Stroke Engines by Applying the Activated Radical Combustion* 2-7

Kalghatgi, G. (2003) *A Method of Defining Ignition Quality of Fuels in HCCI Engines,* SAE 2003-01-1816 3-8

Kaneko, N., Ando, H., Ogawa, H. and Miyamoto, N. 2002. *Expansion of the Operating Range with In-Cylinder Water Injection in a Premixed Charge Compression Ignition Engine.* SAE 2002-01-1743 2-6

Kawanabe, H., Ishiyama, T. and Fujiwara, N. 2004. *Analysis of Premixed Charge Compression Ignition Combustion Using PDF Method with Multidimensional CFD, SAE 2004-01-1913* *2-16*, 3-5

Kontarakis, G., Collings, N., and Ma, T. 2000. *Demonstration of HCCI Using a Single Cylinder Four-Stroke SI Engine with Modified Valve Timing.* SAE 2000-01-2870 2-16

Leppard, W.R., 1990. *The Chemical Origin of Fuel Octane Sensitivity.* SAE 902137 2-11

Livengood,J.C. and Wu, P.C. 1955. *Correlation of Autoignition Phenomena in Internal Combustion Engines and Rapid Compression Machines.* Fifth Symposium (Int.) on Combustion, Reinholds Publishing Corp., p. 347 2-12

Marriott et al., 2002b. *Investigation of Hydrocarbon Emissions from a Direct Injection Gasoline Premixed Charge Compression Ignited Engine.* SAE 2002-01-0419 2-7

Marriott, C. and Reitz, R. 2002a. *Experimental Investigation of Direct Injection Gasoline for Premixed Compression Ignited Combustion Phasing Control.* SAE 2002-01-0418 2-7

Milovanovic, N., Chen, R. and Turner, J. 2004. *Influence of the Variable Valve Timing Strategy on the Control of a Homogeneous Charge Compression Ignition (HCCI) Engine.* SAE 2004-01-1899 2-3

Nakagome, K., Shimazaki, N., Miimura, K. and Kobayashi, S. 1997. *Combustion and Emissions Characteristics of Premixed Lean Diesel Combustion Engine.* SAE 970898 2-7

National Bureau of Standards , 1971. *JANAF Thermodynamic Tables*. 2nd ed. United States Department of Commerce., Washington, DC: USDPO 3-2

Ng, C.K.W and Thomson, M.J. 2004. *A Computational Study of the Effect fo Fuel Reforming, EGR and Initial Temperature on Lean Ethanol HCCI Combustion.* SAE 2004-01-0556 2-9

Noel, L., Maroteaux, F. and Ahmed, A. (2004) *Numerical Study of HCCI Combustion in Diesel Engines Using Reduced Chemical Kinetics of N-Heptane with Multidimensional CFD Code,* SAE 2004-01-1909 2-16, 3-10, 4-13, 4-18

Oakley, A., Zhao, H., Ladommatos, N. and Ma, T. (2001) *Dilution Effects on the Controlled Auto-Ignition (CAI) Combustion of Hydrocarbon and Alcohol Fuels,* SAE 2001-01-3606 4-19

Ogawa, H., Miyamoto, N., Kaneko, N. and Ando, H. (2003) C*ombustion Control and Operating Range Expansion in an HCCI Engine with Selective Use of Fuels with Different Low-Temperature Oxidation Characteristics,* SAE 2003-01-1827 2-8, 4-19

Olsson, J.O., Tunestål, P. and Johansson, B. 2001. *Closed-Loop Control of an HCCI Engine.* SAE 2001-01-1031 2-9

Peng, Z., Zhao, H., and Ladommatos, N. 2003. *Effects of Air/Fuel Ratios and EGR rates on HCCI Combustion of n-Heptane, a Diesel Type Fuel.* SAE 2003-01-0747 2-16

Rabe, T. (2006) *Determination of the Effectiveness of a Hot Tube Igniter to Assist HCCI Combustion.* MSc. Thesis, University of Cape Town. 3-7, 4-1

Rifkin, E.B. and Walcutt, C., 1957. *Basis for Understanding Antiknock Action.* Trans SAE, Vol 65, pp. 552-566 2-11

Risberg, P., Kalghatgi, G. and Ångstrom, H.E. (2003) *Auto-ignition Quality of Gasoline-Like Fuels in HCCI Engines,* SAE 2003-01-3215 3-8

Roelle, M.J., Shaver, G.M. and Gerdes, J. C. 2004. *Tackling the Transition: A Multi-Mode Combustion Model of SI and HCCI for Mode Transition Control,* IMECE 2004-62188 2-16

Stanglmaier, R.H. and Roberts, C.E. 1999. *Homogeneous Charge Compression Ignition (HCCI): Benefits, Compromises, and Future Engine Applications.* SAE 1999-01-3682 2-3, 2-4

Stone, R. (1999) *Introduction to Internal Combustion Engines* (3rd edn.), Great Britain, Macmillan Press Ltd, pg 417- 437 3-1, 3-8

Swarts, A., Yates, A.D.B., Viljoen, C. and Coetzer, R. 2004. *Standard Knock Intensity Revisited: A Typical Burn Rate Characteristics Identified in the CFR Octane Rating Engine.* SAE 2004-01-1850 2-16

Takeda, Y., Keiichi, N. and Keiichi, N. 1996. *Emission Charateristics of Premixed Lean Diesel Combustion with Extremely Early Staged Fuel Injection.* SAE 961163 2-7

Tanaka, S., Ayala, F., Keck, J.C. and Heywood, J.B. 2003. *Two-Stage ignition in HCCI Combustion and HCCI Control by Fuels and Additives,* Combustion and Flame, 132 (2003) 219-239 2-9

Tao, F. and Chomiak, J., 2002. *Numerical Investigation of Reaction Zone Structure and Flame Liftoff of DI Diesel Sprays with Complex Chemistry.* SAE 2002-01-1114 2-10

Thring, R.H. 1989. *Homogeneous Charge Compression Ignition (HCCI) Engines.* SAE 892068 2-7

U.S. Department of Energy, Energy Efficiency and Renewable Energy Office of Transportation Technologies (2001) *Homogeneous Charge Compression Ignition (HCCI) Technology,* April 2001: A Report to the U.S. Congress 2-1, 2-2

Velji, A., Wagner, U., Wiemer, S. and Spiecher, U. 2005. *An experimental Study to Assess the Potential of HCCI Combustion with Various Fuels for Light Duty Diesel.* [Presentation], SAE HCCI Symposium, 2005 2-2

Viljoen, C.L., Yates, A.D.B., Swarts, A., Balfour, G. and Möller, K. 2005. *An Investigation fo the ignition Delay Character of Different Fuel Components and an Assessment of Various Autoignition Modelling Approaches,* SAE 2005-01-2084 2-12, 3-8

Warnatz, J., 2000. *Hydrocarbon Oxidation High-Temperature Chemistry.* Pure Application Chemistry, Vol. 72, No. 11, pp. 2101 2-11

Westbrook, C.K., Warnatz, J. and Pitz, W.J. 1988. *A Detailed Chemical Kinetic Reaction Mechanism for the Oxidation of iso-Octane and n-Heptane over an Extended Temperature Range and its Application to Analysis of Engine Knock.* Twenty-second Symposium (Int.) on Combustion, The Combustion Institute, pp. 893-901 2-11

Xu, H., Fu, H., Williams, H. and Shilling, I. 2002. *Modelling Study of Combustion and Gas Exchange in a HCCI (CAI) Engine,* SAE 2002-01-0114 2-1

Yamasaki, Y. and Iida, N. 2000. *Numerical Simulation of Autoignition and Combustion of n-Butane and Air Mixtures in a 4 Stroke HCCI Engine by Using Elementary Reactions,* SAE 2000-01-1834 3-10

Yao, M., Zheng, Z., Zhang, B. and Chen, Z. (2004) *The Effect of PRF Fuel Octane Number on HCCI Operation,* SAE 2004-01-2992 4-21

Yates, A.D.B., Swarts, A. and Viljoen, C.L. (2005) *Correlating Auto-Ignition Delays and Knock-Limited Spark-Advance Data for Different Types of Fuel,* SAE 2005-01-2083 3-5

Yates, A.D.B., Viljoen, C.L. and Swarts, A. 2004. *Understnding the Relation Between Cetane Number and Combustion Bomb Ignition Delay Measurements,* SAE 2004-01-2017 2-14

Zhao H. 2005. *Systematic Study on CAI/HCCI Combustion Engine,* [Presentation], SAE HCCI Symposium, 2005 2-3

Zhao, F., Asmus, T.W., Assanis, D.N., Dec, J.E., Eng, J.A. and Najt, P.M. 2003. *Homogeneous Charge Compression Ignition (HCCI) Engine – Key Research and Development Issues,* Warrendale, Society of Automotive Engineers passim

APPENDICES

A. Engine Model Details

A.1 Combustion Thermodynamics

The idealised combustion of the fuel-air mixture under non-stoichiometric conditions can be described by the following general reaction:

$$C_xH_yO_z + fO_2 + gN_2 \rightarrow aCO_2 + bH_2O + cCO + dH_2 + eO_2 + gN_2 \qquad \text{(A-1)}$$

Reactants Products

Where, the parameters, a to g, are used to balance the equation. The reaction is classified into reactants[2] and combustion products[3].

In all the reactions N_2 was assumed to be inert, which means that it does not participate in any reaction. In addition, all the reactant and product molecules were assumed to be ideal gases so that the ideal gas law could be applied. Since the temperature of combustion products are normally high, some equilibrium reactions such as the dissociation of CO_2 and the water-gas shift reaction were included, giving rise to the formation of CO and H_2:

$$CO + \frac{1}{2}O_2 \Leftrightarrow CO_2 \qquad \text{(A-2)}$$

$$CO_2 + H_2 \Leftrightarrow CO + H_2O \qquad \text{(A-3)}$$

The thermodynamic equilibrium and Daltons' law of additive pressures[4] governed the rates of the two equilibrium reactions. The equations for calculating the rate constants and all the other thermodynamic properties required are discussed in details by Heywood (1988).

[2] Reactants are on the left of the combustion reaction equation.

[3] Products are on the right side of the combustion reaction equation.

[4] The pressure of a gas mixture is equal to the sum of the pressures each gas would exert if it existed alone at the mixture temperature and volume (Çengel and Boles, 2002).

A.2 Model Operation

The ignition delay model was applied in the combustion model according to the flow-chart given in Figure A-1 for the prediction of the start of main heat release. The engine model was operated according to the flow-chart given in Figure A-2 for the prediction of the engine performance.

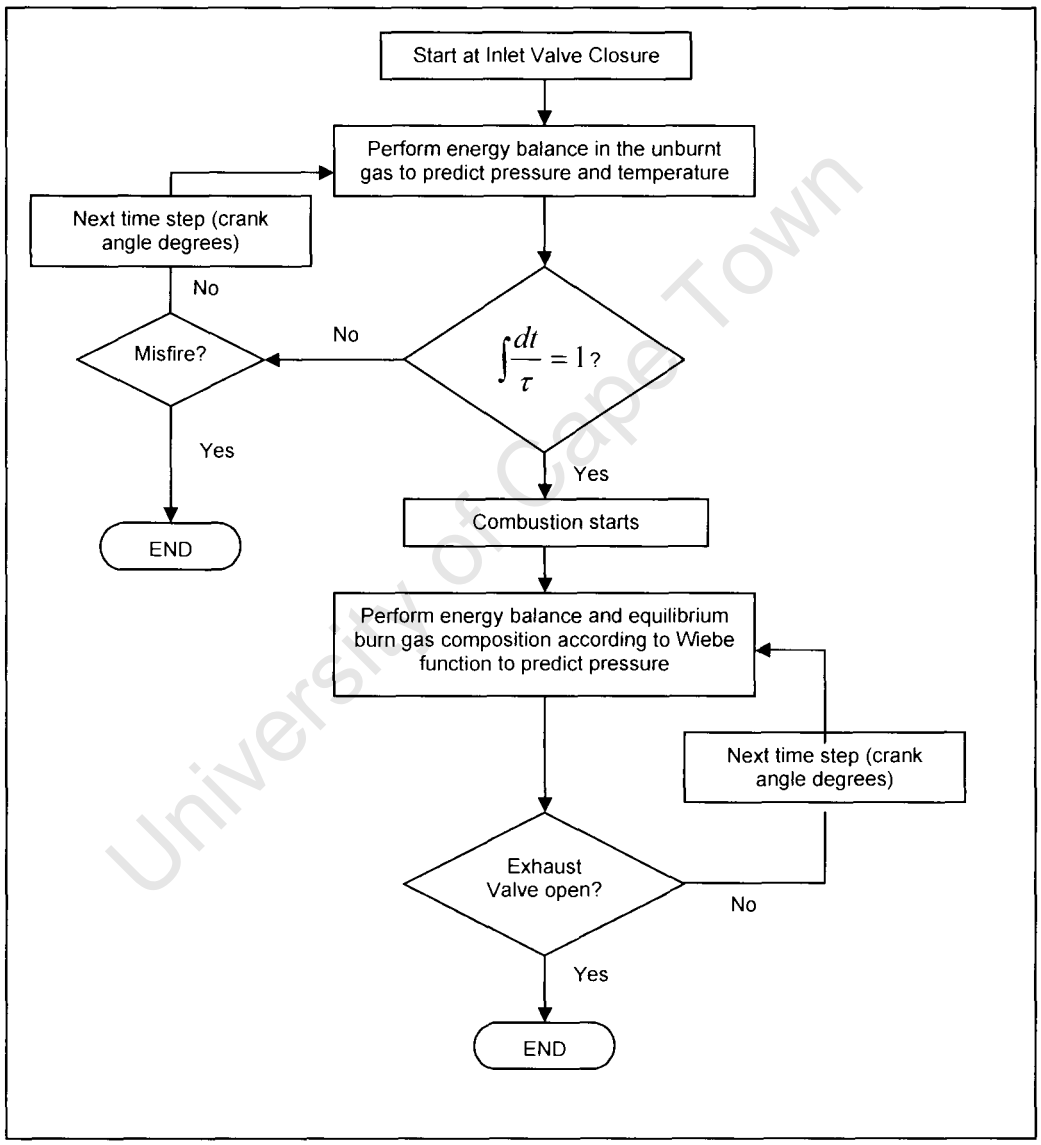

Figure A-1: Flow diagram for the combustion model by incorporation of the ignition delay model with the engine model

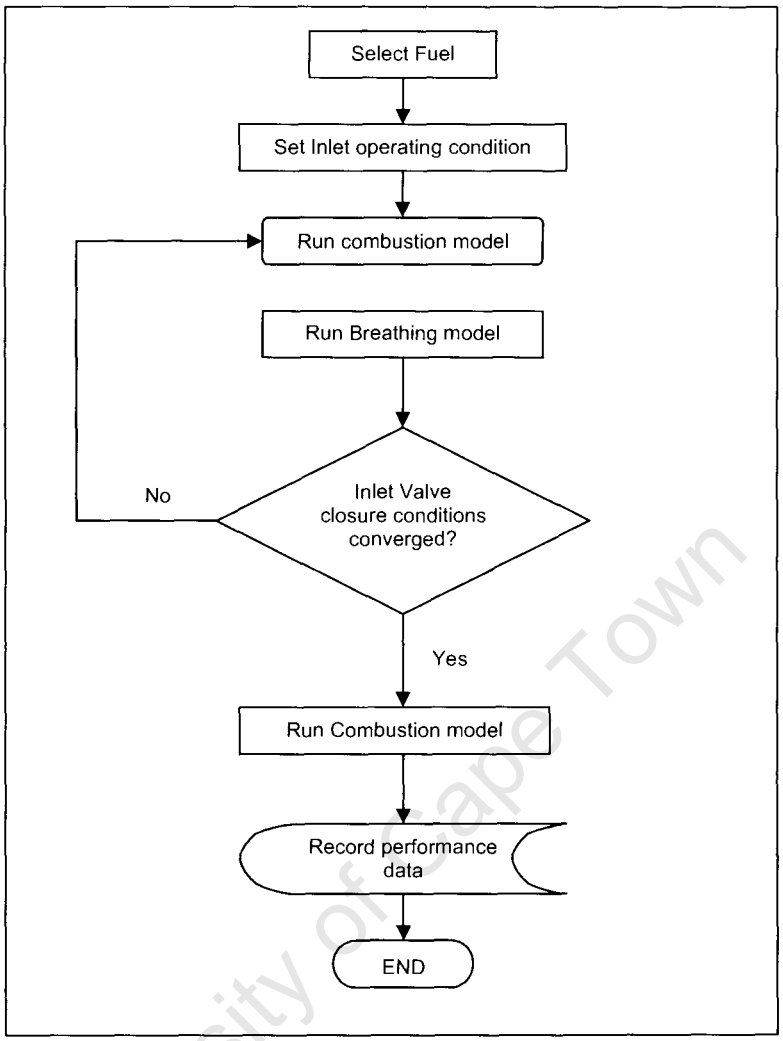

Figure A-2: Flow diagram for the operation of the engine cycle model

References A

Çengel, Y.A. and Boles, M.A. 2002. *Thermodynamics: An Engineering Approach* (4th Edn.). New York, McGraw-Hill Companies, A-2

Heywood, J.B. 1988. *Internal Combustion Engine Fundamentals* (International Edn.). Singapore, McGraw-Hill Book Company A-1, A-2

B. Chemkin Results

Ignition delay values were calculated for a range of primary reference fuels (PRF) over a wide range of pressure, fuel-air equivalence ratio (Φ) and exhaust gas recirculation using a detailed chemical kinetic model. The chemical reaction scheme developed by Westbrook and co-workers for PRF was used (Westbrook et al., 1988). Two separate studies were conducted on the effect of equivalence ratio on ignition delay and the effect of exhaust gases on ignition delay. These studies were conducted so that the overall ignition delay obtained from the 3-part Exponential model for stoichiometric mixture, can be corrected accordingly. The results obtained are shown the following figures.

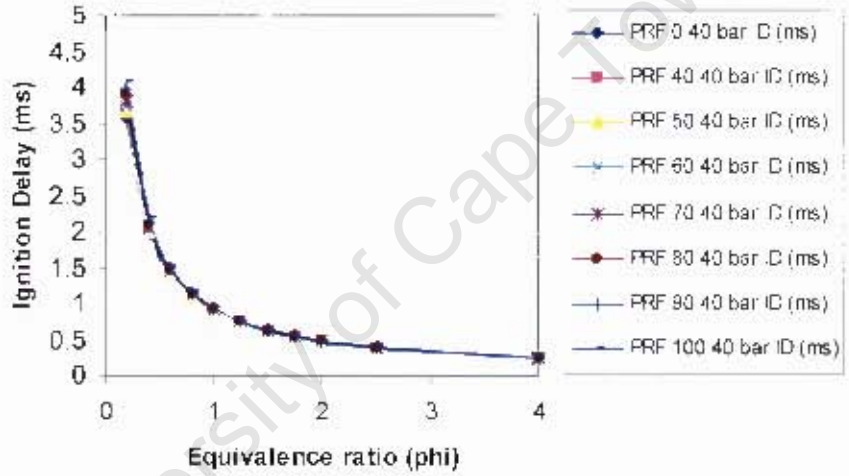

Figure B-1: Effect of equivalence ratio on ignition delay of PRF at 40 bar, 1000 K initial temperature

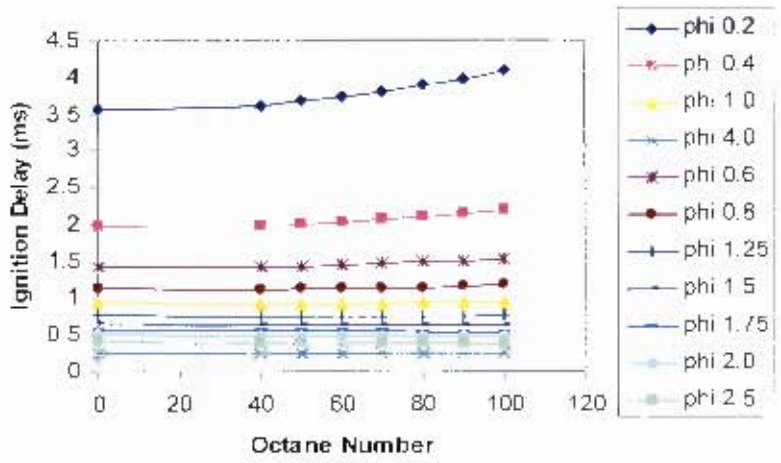

Figure B-2: Effect of the octane number of PRF on ignition delay at 40 bar, 1000 K initial temperature

From these results, an excellent correlation was obtained by fitting a simple power law of the form:

$$\tau_i = \tau_{\lambda=1} \lambda^{\beta} \qquad \text{(B-1)}$$

Typical ignition delay results obtained from this equation are shown in figures B-3 at 40 bar.

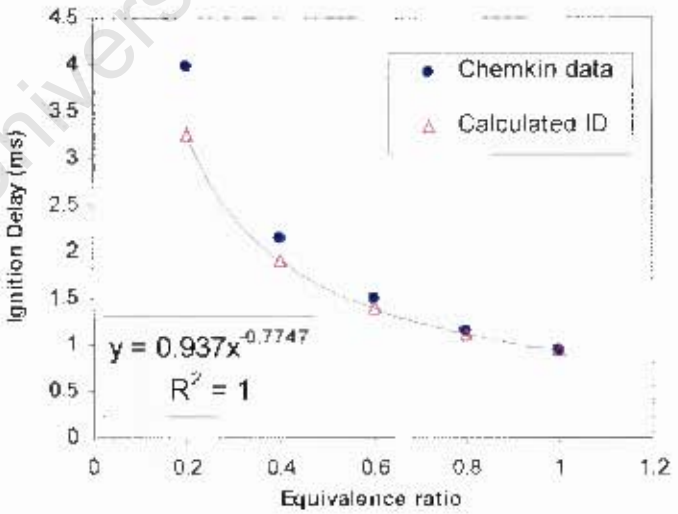

Figure B-3: Comparison of the Chemkin and model ignition delay for PRF 90 at 40 bar, 1000 K initial temperature

The effect of EGR could not be investigated separately from equivalence ratio, since dilution affects the mixture equivalence ratio. Therefore, a distinction was made between the inlet mixture equivalence ratio and the in-cylinder equivalence ratio. The cylinder equivalence ratio was determined from the inlet equivalence ratio and the amount of EGR used. The following figures show the results of the effects of EGR on ignition delay.

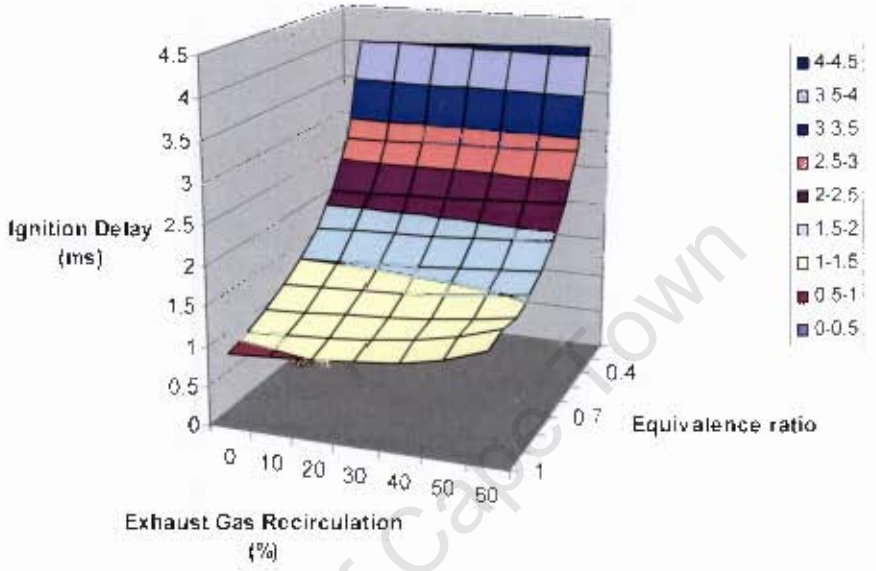

Figure B-4: Effect of EGR on ignition delay for a given equivalence ratio at 40 bar, 1000 K initial temperature for PRF 90

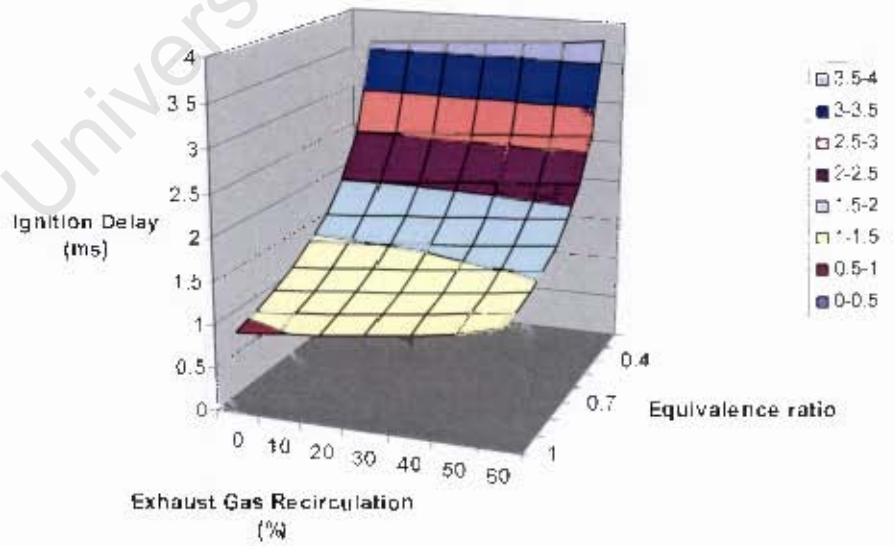

Figure B-5: Effect of EGR on ignition delay for a given equivalence ratio at 40 bar, 1000 K initial temperature for PRF 0

Similar graphs were obtained for all PRF used, least-squares regression analysis was used to map this data onto the ignition delay correlation similar to the one suggested by Gray III and Ryan III (1997), of the form :

$$\tau_i = \tau_{\lambda=1}[F]^a \cdot [O]^m \qquad \text{(B-2)}$$

Where [*F*] and [*O*] are the fuel and oxygen concentrations, respectively. However, the resulting correlation was very poor and an alternative correlation was attempted, of the form:

$$\tau_i = \tau_{\lambda=1}\lambda^k\left(1 - \frac{\%\ EGR}{100}\right)^m \qquad \text{(B-3)}$$

Where, %EGR is the percentage of exhaust gas recirculation on mass basis. This correlation includes the effect of equivalence ratio that was discussed above.

The results from this correlation were comparable with the Chemkin data, however, different values of the parameter, m, were obtained at each equivalence ratio. Figure B-6 shows how the inlet equivalence ratio affects the EGR index, m.

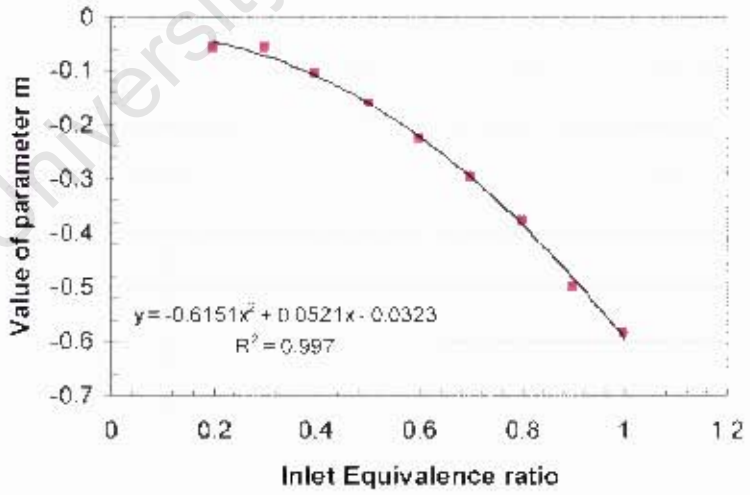

Figure B-6: Effect of inlet equivalence ratio on the EGR index, m

References B

(Bill) Gray, III, A.W. and Ryan, III, T.W. (1997). *Homogeneous Charge Compression Ignition (HCCI) of Diesel Fuel.* SAE 971676 B-4

Westbrook, C.K., Warnatz, J. and Pitz, W.J. 1988. *A Detailed Chemical Kinetic Reaction Mechanism for the Oxidation of iso-Octane and n-Heptane over an Extended Temperature Range and its Application to Analysis of Engine Knock.* Twenty-second Symposium (Int.) on Combustion, The Combustion Institute, pp. 893-901 B-1

C. Fuel Characterisation

Ignition delay parameters for the 3-part Exponential model were obtained from a study by Yates et al. (2005) for the various model fuel components. These parameters describe the autoignition characteristics of the fuels over a wide range of pressure and temperature for a stoichiometric mixture. Table C-1 show the ignition delay parameters of the model fuels, including the parameters of the design fuel.

Fuel	Ln(A1)	n1	B1	Ln(A2)	n2	B2	Ln(A3)	n3	B3
n-Heptane	-18.69	-0.078	14721	18.52	-2.082	-10263	-12.48	-0.927	16441
iso-Octane	-18.86	-0.073	15678	25.92	-2.969	-10595	-10.23	-1.017	13956
1-Hexene	-21.69	-0.081	16719	8.87	-1.436	-2513	-12.85	-0.824	17148
Toluene	40	0	0	40	0	0	-11.52	-0.967	17333
Methanol	40	0	0	40	0	0	-16.01	-0.736	19701

Table C-1: Ignition delay parameters for the different model fuels including the design fuel

Figure C-1 show the autoignition characteristics of the model fuels, including the model blend. Toluene and methanol have single-stage ignition, whereas n-heptane, iso-octane, 1-hexene and the model blend have two-stage ignition.

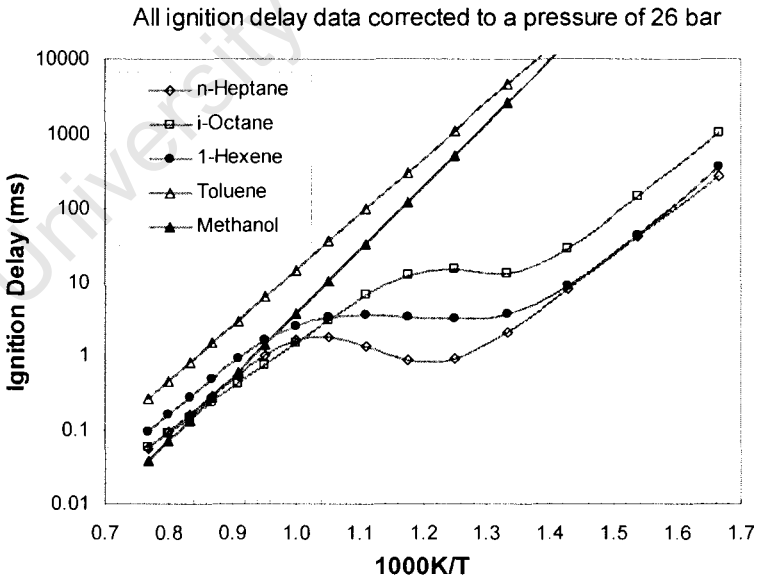

Figure C-1: Autoignition behaviour of model fuels at 26 bar

References C

Yates, A.D.B., Swarts, A. and Viljoen, C.L. (2005) Correlating Auto-Ignition Delays and Knock-Limited Spark-Advance Data for Different Types of Fuel, SAE 2005-01-2083 C-1